Energ. Ecol. Environ. (2023) 8(3):211–240
https://doi.org/10.1007/s40974-023-00271-y

ORIGINAL ARTICLE

A comprehensive experimental study of municipal solid waste (MSW) as solid biofuel and as composite solid fuel in blends with lignite: quality characteristics, environmental impact, modeling, and energy cover

Agapi Vasileiadou[1,2] · **Stamatis Zoras**[1] · **Argiro Dimoudi**[1]

[1] Department of Environmental Engineering, Faculty of Engineering, Democritus University of Thrace, 67100 Xanthi, Greece
[2] Department of Mineral Resources Engineering, University of Western Macedonia, 50100 Kozani, Greece

Received: 29 November 2022 / Revised: 8 February 2023 / Accepted: 10 February 2023 / Published online: 2 March 2023

Abstract Recently, coal power plants across Europe have been reopened. Alternative fuels are needed for energy autonomy purposes, for a smoother transition to the post-lignite era and for sustainable development. In this work, different categories of municipal solid wastes (MSW) and their blends with lignite were studied for their potential use as alternative fuels. Seventeen samples were studied using several techniques: gross calorific value (GCV), proximate analysis, ultimate analysis, ion chromatography, ash elemental analysis, thermogravimetric analysis, kinetic modeling and thermodynamic analysis. A determination of empirical chemical formulas was performed. Slagging/fouling potential was evaluated with various indices including modified indices that take into account ash production and GCV. Maximum emission factors were calculated and defined per produced MJ. Also, an environmental footprint index was developed regarding the environmental impact of solid wastes. The GCV experimental results were compared with those of twenty different empirical models. Moreover, several case studies were performed to evaluate the potential of covering the energy demands, with combustion of MSW, in Greece and Europe. The results showed that MSW as a primary/secondary fuel is an attractive solution considering the fact that it boasts better characteristics in comparison with lignite. Moreover, the environmental footprint index (EFI_{sw}) of the MSW revealed a much smaller environmental impact. The high N content is not always translated to high emissions if NO is expressed per produced MJ (gNO/MJ). In addition, MSW can also be used as a significant contributor in covering energy demands regarding the energy recovery potential.

✉ Agapi Vasileiadou
avasileia@env.duth.gr; agvasileiadou@gmail.com

Graphical abstract

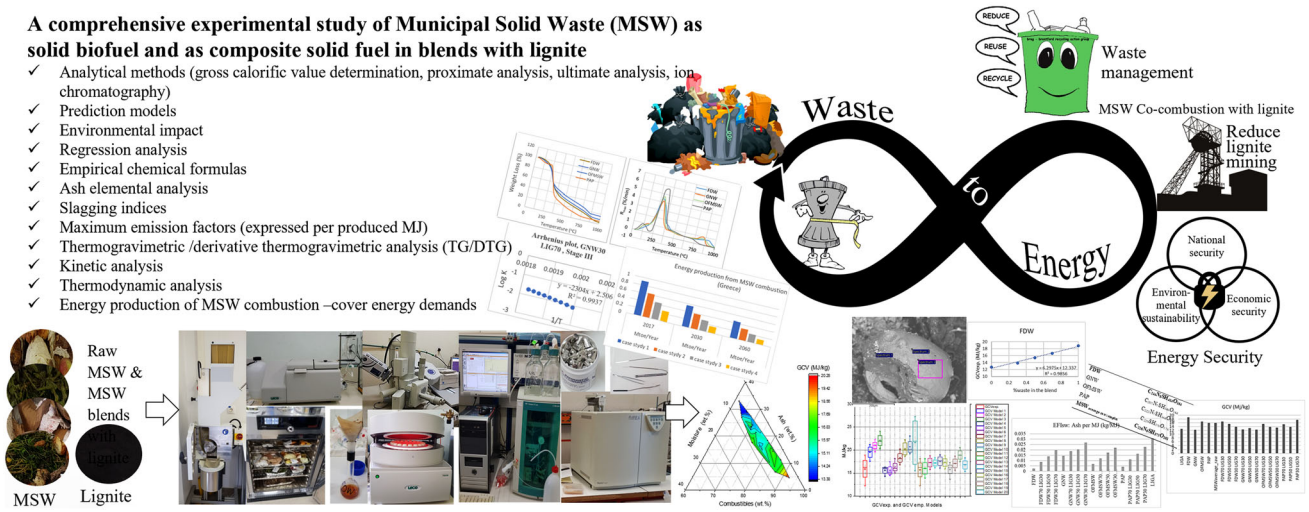

Keywords Co-firing · Emission factors · Kinetic modeling · Municipal solid wastes (MSW) management · Thermochemical conversion · Waste-to-energy (WtE)

1 Introduction

The world is facing serious resource and environmental challenges due to the rapid increase in population and the sharp increase in energy demands and energy prices: Such challenges/problems include climate change, greenhouse gas (GHG) emissions, solid waste management problems, energy crisis, etc. Greece is still dealing with long-term challenges in many environmental issues (e.g., waste management, renewable energy etc.) and recently designed strategies according to the principles of circular economy as well as strategies to face climate change. Greece has not improved its waste management practices in contrast to the improvements made by other members of EU-27. More specifically, in Greece, MSW management still relies on landfilling (80%), while only 15% of MSW is recycled (4th lowest rate among the EU countries), about 4.1% is composted and finally, less than 1.1% of the available MSW is used for energy recovery (Sarigiannis et al. 2021).

Combustion is recognized and considered as a promising and environmentally friendly solution for MSW management, since the energy produced by conversion of MSW is an economically affordable energy source. Biomass co-combustion with coals is an interesting alternative approach that could reduce the environmental impact (decreased CO_2, CH_4, SO_x, NO_x emissions, etc.) in contrast to the exclusive use of fossil fuels (Loo and Koppejan 2008; Vasileiadou et al. 2021a). MSW is a source of biomass; therefore, it is renewable (Al-Qayim et al. 2019). Coal co-combustion of biomass residues/wastes reduces greenhouse gas emissions, since landfilling is avoided (CH_4 is known to have a much higher global warming impact than CO_2). The emissions from MSW combustion are at such low levels, that the United States Environmental Protection Agency regards MSW combustion as a clean source of energy (World Bank 2018). The quality, the quantity and the leachates of MSW vary from one region to another and depend on climate and socio-economic conditions (Zhu et al. 2021). Generally, 93% of waste is dumped in low-income countries while in high-income countries this is only 2%. Globally, approximately 37% of the waste is disposed in landfill, 33% is openly dumped, 19% is recycled and composted, while 11% is treated through modern incineration. (World Bank 2018). Li et al. (2004) studied NO and N_2O emissions (mg/Nm^3) from MSW co-firing with coals (bituminous coal and anthracite) on pilot scale circulating fluidized bed combustion (CFBC) and reported that the increase of the co-firing rates, reduces the N_2O emissions while NO emissions are scarcely affected. Matli et al. (2019) studied the physicochemical characteristics (GCV, in MJ/kg, ash content, in %) and emissions (CO_2, SO_2, NO_x, in kg/d) of MSW co-firing with Indian coal either including the food waste or without food waste and concluded that co-combustion with coal is an efficient process for the utilization of MSW. Similarly, Suksankraisorn et al. (2010) studied the high moisture content of MSW in co-firing with Thai lignite in fluidized bed and concluded that SO_2 emissions are lower for lower waste moisture. Vamvuka et al. (2015) studied blends of 50% urban wastes (MSW and waste paper) and 50% lignite

using several methods including TG/MS analysis and concluded that co-firing of such blends is an attractive approach. In a previous study made by the authors, organic, textiles and paper wastes and their blends with Greek lignite were studied via thermal analysis (Iordanidis et al. 2018). A techno-economic analysis of an oxy-fuel based steam turbine power system using municipal solid waste and coals was performed (Sahu and Prabu 2022).

Perera et al. (2021) prepared a review paper regarding the modeling of the thermochemical conversion of several kinds of biomass waste. Ding et al. (2021) studied the co-combustion behavior of municipal solid waste and low-rank coal semi-coke in air or oxygen/carbon dioxide atmosphere. A methodology for the techno-economic analysis of MSW systems based on a social cost–benefit analysis with an evaluation of externalities was performed by Medina-Mijangos et al. (2021). The energy recovery potential from combustion of MSW based on a multi-scenario analysis in Beijing was studied by Gu et al. (2021). Also, this potential has been studied by using moving grate and circulating fluidized bed technologies by Bourtsalas et al. (2020). A techno-economic analysis of energy generation from waste incineration in Mexico was studied by Escamilla-García et al. (2020). The energy, exergy, and economic (3E) analyses of three scenarios was performed by Alrobaian (2020). The combustion behavior, kinetics, and thermodynamics of fine screenings classified from Chinese MSW were explored by TG-FTIR (Tian et al. 2022). Kinetic analysis of the co-firing of MSW and low-rank coal from Pakistan was investigated by Azam et al. (2020a).

Gross calorific value (GCV) is one of the most important quality characteristics of a fuel. The GCV of a fuel can be determined either experimentally via a bomb calorimeter or theoretically by using proximate or/and ultimate analysis. The formulas proposed by Tillman (1978) and Jiménez and González (1991) are among the oldest models (1978 and 1991) and are based on ultimate analysis and proximate analysis, respectively.

Ash-related problems such as slagging, fouling, and agglomeration are governed by the properties of the ash of the fuel, that is, the composition of ash as well as interactions and positive/negative synergistic effects among the various substances that are present in the ash. For these reasons, several slagging/fouling and agglomeration indices have been developed such as the B/A ratio, slagging/Babcock index Rs, fouling index, Fu, slag viscosity index, Sr (Pronobis 2005), bed agglomeration index, BAI (Bapat et al. 1997). All these very useful indices take into account the elemental composition of the ash and in some cases its synergistic effects are also taken into account, however, they do not take into account either the quantity of the produced ash or the GCV value. An exception is the alkali index, Ai (Miles et al. 1995) that takes into account not only the elemental composition of the ash but also the GCV and the ash content of the fuel.

In general, the combustion of MSW either exclusively or in combination with lignite has been found to be promising in terms of improving GCV value and reducing gas emissions and ash production. Although there are several studies in literature about thermochemical characteristics of MSW (e.g., GCV, ash content, N content, S content, etc.), there is lack of studies that investigate all these characteristics combined in order to contribute to a more objective evaluation of alternative solid biofuels. More specifically, the emissions and the ash production are typically expressed per kg of fuel and not per produced energy, which can provide a more objective assessment of the fuel's environmental impact. Most of the literature studies, as mentioned above, report the results of Ultimate analysis of a fuel in the form of Nitrogen content, Sulfur content etc. The normalized values of emissions, per produced energy, could be a useful tool for an easier classification of fuels. Similarly, slagging indices take into account the chemical composition of ash but not the amount of ash or the GCV. Recently, modified slagging and fouling indices were developed by the authors of this study, which take into account not only the chemical composition of the ash but also the GCV of the fuel and the quantity of produced ash during combustion (Vasileiadou et al. 2022).

Also, regardless of the composition, ash is a secondary solid waste and thus, the amount of produced ash is an important parameter for the evaluation of the environmental impact of a solid fuel. The ash production is readily derived by the proximate analysis or TGA; however, this value is not typically normalized by taking into account the produced energy. For instance, a fuel with a high content of ash and a high GCV has a lower environmental footprint impact compared to a fuel with a high ash content and a low GCV. Moreover, several studies have been reported about the combustion characteristics of MSW and combustion technologies in biomass co-combustion (Iordanidis et al. 2018; Matli et al. 2019; Mushtaq et al. 2020; Vasileiadou et al. 2020, 2021a), but available literature for kinetics and thermodynamic analysis of MSW co-combustion with lignite is very limited. Also, this is the case for reports about the potential cover of energy demands by using MSW as a fuel. Further research is needed in order to gain better understanding of organic wastes with lignite co-combustion behavior. The main scope of this work is to perform a comprehensive and comparative evaluation of four MSW categories (food waste, green waste, organic fraction of MSW and paper waste) and their twelve blends with lignite in terms of: (1) combustion characteristics, (2) maximum gas emissions, (3) secondary waste production

including ash quality and quantity, (4) fouling and slagging potential, (5) kinetic and thermodynamic analysis and (6) examination of various scenarios for the energy demand which could be covered by the combustion of MSW. The main contribution of this study is that the above-mentioned evaluation is based not only in physicochemical characteristics but also in other aspects such as availability and potential energy cover. Also, the physicochemical characterization which includes the environmental impact evaluation is performed by using a new environmental footprint index (EFI) and other tools that were recently developed by authors. Moreover, this study aims to fulfill the scientific gap regarding the evaluation and characterization of MSW and alternative solid composite fuels—MSW blends with lignite (Waste-to-Energy practice, WtE). By using the above-mentioned evaluation tools for solid fuels, alternative solid biofuels (wastes, agricultural residues, blends, etc.) with specific and tuned fuel quality characteristics could be developed and be available in energy market for energy production, helping countries, like Greece, to deal with long-term challenges such as environmental issues, waste management, and energy crisis.

2 Materials and methods

Four different MSW samples, namely FDW—food waste, GNW—green waste, OFMSW—organic fraction of municipal solid wastes, PAP—paper of municipal solid wastes, were collected from the integrated waste management plant in Kozani, Greece. A lignite sample, LIGA, was collected from Agios Dimitrios coal-fired power plant, located in Kozani, in Greece. All samples were air died for two weeks and then dried in a furnace at 80 °C for 24 h. Finally, they were ground to a size lower than 1 mm in a Retsch SM100 cutting mill. For each sample, three different blends were prepared at three proportions of 30 wt.%, 50 wt.% and 70 wt.%. Totally, 17 samples were analyzed. All samples were analyzed at least in two replicates.

The gross calorific value (GCV) of raw fuels and their blends was measured in a bomb calorimeter, Leco AC 500, using the ASTM D5865-13 standard (ASTM International 2013). Furthermore, the GCV of the blends was calculated using Eq. (1) and compared to the GCV experimental values.

$$GCV_{\text{calculated of blends}} = \%\text{waste}GCV_{\text{measured\_raw waste}} + \%\text{lignite}GCV_{\text{measured\_raw lignite}} \quad (1)$$

where %waste is the composition of raw biomass sample in the blend, $GCV_{\text{measured\_raw waste}}$ is the measured (experimental) gross calorific value of raw biomass sample (in MJ/kg), %lignite is composition of lignite in the blend, and $GCV_{\text{measured\_raw lignite}}$ is the measured (experimental) gross calorific value of raw lignite sample (in MJ/kg).

For comparison reasons with lignite sample, seven ΔGCV group categories (< 0%, < 15%, 15.1–30%, 30.1–45%, 45.1–60%, 60.1–75% and 75.1–100%) were created. Lignite sample was used as a reference sample. For example, ΔGCV < 15% is meant for a sample (either raw waste or blend) which has up to 15% higher GCV than the one of lignite.

Several empirical models, see Table 1 and Eqs. (2)–(21), were used, and their values were compared to the experimental results in order to find which models best fit in with the results of this study. Four prediction models were developed for the four categories of MSW (FDW, GNW, OFSMW and PAP) in order to be able to calculate the GCV of MSW blends with lignite from the percentage of MSW in the blend with lignite.

The proximate analysis of every sample was carried out in order to determine the volatile matter, moisture, ash and fixed carbon content, in wt.% using a TGA 701 instrument according to the ASTM D7582 standard (ASTM International 2015).

The ultimate analysis (elemental composition) of the samples was performed via a ThermoFinnigan Instrument, FlashEA 1112 Elemental Analyzer (CHNS). The elemental oxygen (O) content in wt.%, was calculated by difference by the following equation Eq. (22).

$$O = 100 - C - H - N - S - \text{Ash} \quad (22)$$

For the ultimate analysis, dried and powdered sample (about 3–5 mg) was combusted at a temperature of 900 °C using a gas chromatographic column (CHNS/NCS Packed column), and a thermal conductivity detector (TCD). The purity of O_2 which was used for the ultimate analysis was 99.9999%. BBOT ($C_{26}H_{26}N_2O_2S$), sulfanilamide ($C_6H_8N_2SO_2$) and L-Cystine ($C_6H_{12}N_2O_4S_2$) were used as standard compounds.

The anions Cl^- of the samples were determined by a Metrohm Ion Chromatographer, Model 881, Compact IC Pro as described in a previous work (Vasileiadou et al. 2021c).

Empirical chemical formulas were calculated from the results of elemental analysis of the samples as reported in a previous study (Vasileiadou et al. 2021a). Empirical chemical formula of a fuel is the simplest ratio of elements in a compound.

The maximum potential emission factors (CO_2, SO_2 and NO) were calculated from the results of the ultimate analysis and calorific value determination, as applied in a previous study by the authors (Vasileiadou et al. 2021b) and are expressed as grams of emitted gas per 1 MJ of

Table 1 GCV empirical models

Empirical model	Notes	Reference	Equations
$GCV = 99.5C - 136.2H + 61.9O + 143.1N - 1392.6$	Kcal/kg	Kathiravale et al. (2003), Komilis et al. (2012)	(2)
$GCV = 8561.11 + 179.72H - 63.89S - 111.17O - 91.11Cl - 66.94N$	Kcal/kg, MSW	Chang model (Komilis et al. 2012)	(3)
$GCV = 80.3C + 338.9H - 3.47O + 22.49S$	Kcal/kg, Coal / refuse	Mott and Spooner model (Komilis et al. 2012)	(4)
$GCV = 1558.8 + 19.96C + 44.3O - 671.8S - 19.92W$	R2 = 0.926, MSW, Kcal/kg	Liu model (Liu et al. 1996)	(5)
$GCV = 80.5C + 338.6H - 42.3O + 22.2S + 5.55N$	MSW, Kcal/kg	Delong model (modified) (1993) (Komilis et al. 2012)	(6)
$GCV = 81(C - 3(O/8)) + 171(O/8) + 345(H - O/16) + 25S - 6(9H + W)$	MSW, Kcal/kg	Steuer's model (Komilis et al. 2012)	(7)
$GCV = 81(C - 3(O/4)) + 342.5H + 22.5S + 171(O/4) - 6(9H + W)$	MSW, Kcal/kg	Scheurer and Kestner's model (Liu et al. 1996)	(8)
$GCV = 85.1VM - 1671.9$	Kcal/kg		(9)
$GCV = 85.1VM - 28.2FC - 1337$	Kcal/kg		(10)
$GCV = 0.916 \cdot FC + 14.119$	MJ/kg, Biomass, error Mean diff. 2.20%	Demirbas Model (Parikh et al. 2005)	(11)
$GCV = -10814.08 + 313.3(FC + VM)$	Kcal/kg, errors $< 10\%$, lignocellulosic residues	Jimenez and Gonzalez model (1991) (Jiménez and González 1991)	(12)
$GCV = -10.216 + 0.621C$	MJ/kg, biomass	Toscano model (Toscano et al. 2013)	(13)
$GCV = -1.3675 + 0.3137C + 0.7009H + 0.0318O$	MJ/kg, biomass, R2 = 0. 834, $\pm$ 5% error	Sheng and Azevedo (2005) (Toscano et al. 2013)	(14)
$GCV = 0.3259C + 3.4597$	MJ/kg, biomass, R2 = 0.758, $\pm$ 5% error	Sheng and Azevedo (2005) (Toscano et al. 2013)	(15)
$GCV = -0.763 + 0.301C + 0.525H + 0.064O$	MJ/kg, R2 = 0.792	Sheng and Azevedo (2005)	(16)
$GCV = 0.32(C + 2H)$	MJ/kg, biomass	Toscano model (Toscano et al. 2013)	(17)
$NCV = 44.75 \cdot OM - 5.85 \cdot M + 21.2$	MSW, Kcal/kg	Bento's Model (Abu-Qudais and Abu-Qdais 2000)	(18)
$GCV = -2.032 + 0.4537C$	Biomass, MJ/kg	Toscano model (Toscano et al. 2013)	(19)
$GCV = 0.971 + 0.326C + 0.711H$	Biomass, MJ/kg	Toscano model (Toscano et al. 2013)	(20)
$GCV = 0.4373C - 1.6701$	Wood and bark	Tillman model (Tillman 1978)	(21)

where C: carbon, H: hydrogen, O: oxygen, N: nitrogen, S: sulfur, Cl: chlorine, M or W: water (moisture content), VM: volatile matter, FC: fixed carbon, OM: organic matter (in wt%)

produced energy. SO_2 emissions were studied / expressed as SO_2 which represent approximately 95% of sulfur-containing product emissions while only a very small percentage of SO_2, less than 5%, is oxidized to SO_3 (Hupa et al. 2017). Moreover, nitrogen-related emissions were expressed as nitrogen monoxide (NO) emissions since more than 90% of nitrogen is converted to NO and less than 10% is converted to NO_2 (Loo and Koppejan 2008).

Thermogravimetric—derivative thermogravimetric analysis (TG/DTG) was performed by using a TGA 701 LECO device, according to Vasileiadou et al. (2021c) in order to obtain the thermogravimetric characteristics: the ignition temperature, T_i which is the temperature at which combustion initiates after dehydration, the burnout temperature, T_b, that is the temperature at which the combustion ends with no further weight loss. Also, from the TG profiles of the samples, the temperature at which there is the maximum rate of weight loss ($R_{\max}$), $T_{\max,}$ as well as the duration of combustion, t_b was determined. Furthermore, the theoretical DTG profiles of the samples were calculated using Eq. (23) (Peng et al. 2015).

$$\text{Theoretical DTG} = (\mathrm{d}w/\mathrm{d}t)_{\text{samp1}} \cdot x_1 + (\mathrm{d}w/\mathrm{d}t)_{\text{samp2}} \cdot x_2 \tag{23}$$

where x_1 and x_2 are the content (mass fraction) of sample 1 and 2, respectively, which take part in the fuel mixture, dw/dt is the first derivative of the weight loss of samples 1 and 2.

The theoretical DTG curves (1st derivative weight loss %/min as a function of temperature) were compared with the corresponding experimental ones, in order to identify any synergistic effects.

Kinetic analysis was applied for modeling the decomposition kinetics of the analyzed samples and MSW blends with lignite, as described in a previous study of the authors (Vasileiadou et al. 2021a). With this method, kinetic parameters such as activation energy, E, and pre-exponential factor, A, were determined by using the TG/DTG data and the TG/DTG profiles of analyzed samples and blends (MSW and lignite) and the Arrhenius equation, Eq. (24). TG/DTG profiles of every sample were divided into temperature ranges, each one corresponding to a different stage of the overall reaction. Stage I and II were associated to dehydration. The combustion initiates at the beginning of stage III and ends at the peak temperature ($T_{\max}$) which corresponds to the maximum rate of weight loss ($R_{\max}$), based on the DTG profiles. The combustion kinetics can be described by a first order kinetics equation, Eq. (24) (Cumming 1984):

$$K = A \cdot \exp(-E/R \cdot T) \rightarrow \log K = \log A - E/2.303 \cdot R \cdot T \tag{24}$$

and $K = -(\mathrm{d}W/\mathrm{d}t)/W$, where E is the activation energy, kJ/mol, K is the specific reaction rate, A is the pre-exponential factor (frequency factor), s^{-1}, R is the universal gas constant (8.314 JK^{-1} mol^{-1}), T is the instantaneous absolute temperature, K. Equation (24) can be expressed as Y = aX + b, where a, b is the slope and intercept of Arrhenius plot (1/T versus logK) of stage III of the analyzed samples and MSW blends with lignite.

The thermodynamic analysis was performed, as described in a previous study of authors (Vasileiadou et al. 2021a) in order to calculate Enthalpy change (ΔH_α, kJ mol^{-1}), Gibbs free energy change (ΔG_α, kJ mol^{-1}) and entropy change (ΔS_α, kJ $mol^{-1}K^{-1}$) from Eqs. (25) to (27):

$$\Delta H_\alpha = E_\alpha - R \cdot T_\alpha \tag{25}$$

$$\Delta G_\alpha = E_\alpha + R \cdot T_m \cdot \ln(K_B * T_m/h \cdot A) \tag{26}$$

$$\Delta S_\alpha = (\Delta H_a - \Delta G_a)/T_m \tag{27}$$

where R is the Universal gas constant, 8.314 JK^{-1} mol^{-1}, T_α is the final temperature of stage III, in K, K_B is the Boltzmann constant, 1.3819E-23 JK^{-1}, h is the Plank's constant, 6.6269E-34 Js, T_m is the peak temperature, K (see DTG profiles).

Scanning electron microscope and energy-dispersive spectroscopy (SEM JEOL JSM-6390LV-EDS, INCA 300) were performed as described in a previous study of the authors (Vasileiadou et al. 2022). The main elements in the blends were calculated theoretically, with the following procedure: Firstly, the composition of the raw fuel (either lignite or biomass sample) was calculated for any desired element, e.g., Ca by taking into account the ash content of the raw fuel and the composition of the ash in the desired element. More specifically, from the results of SEM–EDS it was concluded that ash from the lignite sample has 26.59% Ca and from the proximate analysis it is known that lignite has 38.90% ash. In 100 g of ash, 26.59 g of Ca are contained. It follows that in 38.90 gr of ash, corresponding to 100 gr of raw lignite, X = (38.9*26.59)/100 = 10.34 g of Ca will be contained. For the raw biomass sample, the same procedure was followed and the g of Ca contained in 100 g of raw fuel are equal to Y. Since these elements are involved in inorganic substances that are not volatile, it follows that in 100 g of a blend of 30% lignite and 70% biomass, Z = (0.3*X + 0.7*Y) g of Ca will be contained. By taking into account the ash of the blend, e.g., 10%, then the composition of the ash of the blend was estimated as follows: In100 g of blend fuel, corresponding to 10 g of ash, Z g of Ca is contained. It follows that in 100 g of the ash of this blend there are V = 100*Z/10 g of Ca.

Several ash indices, basic to acid compound (B/A) index, bed agglomeration index (BAI), Babcock index–

slagging index (Rs), fouling index (Fu), and slag viscosity index (Sr) were calculated as described in previous study of authors (Vasileiadou et al. 2022).

The novel modified ash indices were calculated according to a previous study by the authors (Vasileiadou et al. 2022). Briefly, in the modified indices besides the quality of ash in terms of its composition, also, the quantity of the produced ash and the produced energy are taken into account.

Various scenarios were developed regarding waste-to-energy (WtE) in order to evaluate the potential cover of energy demand. The variables that were used are presented in Table 2.

Also, the results of GCV of MSW in this study (Vasileiadou et al. 2022) (the average value of GCV of the samples FDW, GNW, OFMSW and PAP was about 15.92 MJ/kg) were used for the calculations. The percentage of MSW which refers to FDW, GNW, OFMSW and PAP is 54.6%. For the years 2017, 2030 and 2060, it was assumed that 10.7% of wastes were composted and thus cannot be used for combustion. The population in millions of Greece and Europe, was also used for the calculations and were considered to be increased in 2030 and 2060 by 13% and 36%, respectively, compared to the population of the year 2017 (reference year) (OECD 2018).

The waste generation (in kg/capita/year, and in million tonnes per year) was also used.

The primary energy production was used, specifically, the actual data for the year 2017 (reference year), and a forecast for the year 2030 and 2060 as follows:

2.1 For Greece

- Scenario I. 7.5 Mtoe/year, year 2017 (total production of primary energy) (Eurostat 2019)
- Scenario II. 8.48 Mtoe/year, forecast for the year 2030 (OECD 2018),
- Scenario III. 10.20 Mtoe/year, forecast for the year 2060), in Mtoe/year (OECD 2018).

2.2 For Europe

- Scenario I. 758.2 Mtoe/year, given year 2017,
- Scenario II. 856.8 Mtoe/year, forecast for the year 2030 (OECD 2018),
- Scenario III. 1031.2 Mtoe/year, forecast for the year 2060), in Mtoe/year (OECD 2018).

Table 2 Variables used for the developed case studies in WtE

	Scenario 1 (year 2017):	Scenario 2 (forecast for year 2030):	Scenario 3 (forecast for year 2060):
Greece's primary energy production (Mtoe/year)	7.5 where the 60.9% produced from solid fossil fuels[a]	8.48 (+ 13%)	10.20 (+ 36%)
EU primary energy production (Mtoe/year)	758.2 where the 16.4% is produced from solid fossil fuels[a]	856.8 (+ 13%)	1031.2 (+ 36%)
Population in Greece (in millions)	10.77[b]	12.17 (+ 13%)[d]	14.65 (+ 36%)[d]
Population in EU (in millions)	511.8	578.3 (+ 13%)[d]	696.0 (+ 36%)[d]
EU-28 Waste generation (kg/capita/day)	1.18[c]	1.30[c]	1.45[c]
Waste generation in Greece (kg/capita/year)	503.7[c]	491.1	547.70
Waste generation in EU (kg/capita/year)	430.7	474.5	529.3
Food waste, green waste and paper waste, in %	54.6[c]	54.6	54.6
Share of Composting (Waste treatment in EU) in %	10.7[c]	10.7	10.7
MSW which will be used (in this study) for energy production in Greece (54.6% of MSW—10.7% compost), (kg/capita/year)	221.1	120.8	79.97
MSW which will be used (in this study) for energy production in EU of MSW (54.6% of MSW—10.7% compost), (kg/capita/year)	189.1	116.7	77.3

[a](Eurostat 2019), [b](Eurostat 2020), [c](World Bank 2018), [d](OECD 2018)

3 Results and discussion

3.1 Energy content, regression analysis and comparison of the experimental GCV with several empirical models

3.1.1 Energy content of the MSW samples and MSW blends with lignite

Gross calorific value is one of the major quality characteristics of a fuel, and it is translated to the amount of heat that a fuel releases during combustion. The GCV results of raw MSW, their blends with lignite, and lignite sample (LIGA sample) (reference sample) are illustrated in Table 3. The %difference of GCV of every sample in comparison with GCV of LIGA sample was calculated as described in a previous study of the authors (Vasileiadou et al. 2021b). ΔGCV_{sample} is the difference between the GCV of every sample (GCV_{sample}) and the GCV of lignite sample (GCV_{LIGA}). Several group categories were created in order to categorize fuels in accordance to lignite GCV: [< 0%], [< 15%], [15.1–30%], [30.1–45%], [45.1–60%], [60.1–75%], [75.1–90%] and [> 90.1%].

The GCV of a sample should be greater than 7.94 MJ/kg in order to be considered as fuel (Azam et al. 2020b). All analyzed samples and blends revealed higher GCV than the above-mentioned value. More specifically, raw samples exhibit higher gross calorific value than lignite (12.68 MJ/kg) except for the GNW sample (12.23 MJ/kg). FDW revealed the highest GCV ($\sim 19 \pm 0.13$ MJ/kg, ΔGCV: + 49%) among raw samples. Boumanchar et al. (2018) concluded that the GCV of food wastes varied from 4 MJ/kg to 38.3 MJ/kg, with a standard deviation of ± 10.3 (result of 187 MSW). High calorific value of the samples is related to the low percentage of moisture content and to the high percentage of volatiles.

In general, the quality of MSW as expressed by its composition and the quantity of MSW are influenced by various factors, such as socio-economic factors of every region, population, income per capita, and human work. Similar results for the PAP sample have been reported for MSW of the island of Crete (Gidarakos et al. 2006).

In FDW and OFMSW blends with lignite, as the percentage of waste is increased in blends with lignite, the GCV is also increased. In GNW and PAP blends with lignite this is not the case, most likely due to poor mixing

Table 3 Gross calorific value of raw MSW samples, their blends with lignite, and lignite (as a reference), in different proportions 30 wt.%, 50 wt.%, 70 wt.%

Sample ID	$GCV_{experimental}$ (MJ/kg)	$GCV_{calculated\ of\ blends}$	*%Deviation between* $GCV_{exp.\ and}$ $GCV_{theor.\ of\ blends}$	*ΔGCV (%)*	*ΔGCV* Group category
LIGA[1]	12.68 ± 0.11	–	–	–	–
FDW	18.87 ± 0.13	–	–	48.79	[45.1–60%]
GNW	12.23 ± 0.84	–	–	− 3.58	[< 0%]
OFMSW	16.62 ± 0.33	–	–	31.08	[30.1–45%]
PAP	15.98 ± 0.11	–	–	26.01	[15.1–30%]
$MSW_{average\_raw}$	15.92 ± 0.35	–	–	25.59	[15.1–30%]
FDW70 LIG30	16.64 ± 0.23	17.01	− 2.21	31.19	[30.1–45%]
FDW50 LIG50	15.39 ± 0.12	15.77	− 2.43	21.37	[15.1–30%]
FDW30 LIG70	13.85 ± 0.28	14.54	− 4.70	9.25	[< 15%]
GNW70 LIG30	12.47 ± 0.36	12.36	0.86	− 1.66	[< 0%]
GNW50 LIG50	13.11 ± 0.47	12.45	5.28	3.40	[< 15%]
GNW30 LIG70	12.36 ± 0.35	12.54	− 1.50	− 2.56	[< 0%]
OFMSW70 LIG30	15.32 ± 0.11	15.44	− 0.81	20.77	[15.1–30%]
OFMSW50 LIG50	13.77 ± 0.05	14.65	− 5.99	8.62	[< 15%]
OFMSW30 LIG70	13.40 ± 0.06	13.86	− 3.33	5.68	[< 15%]
PAP70 LIG30	15.12 ± 0.42	14.99	0.90	19.27	[15.1–30%]
PAP50 LIG50	13.75 ± 0.16	14.33	− 4.06	8.42	[< 15%]
PAP30 LIG70	17.46 ± 0.11	13.67	27.72	37.69	[30.1–45%]

GCV of LIGA sample was studied in a previous work of the authors (Vasileiadou et al. 2021b)

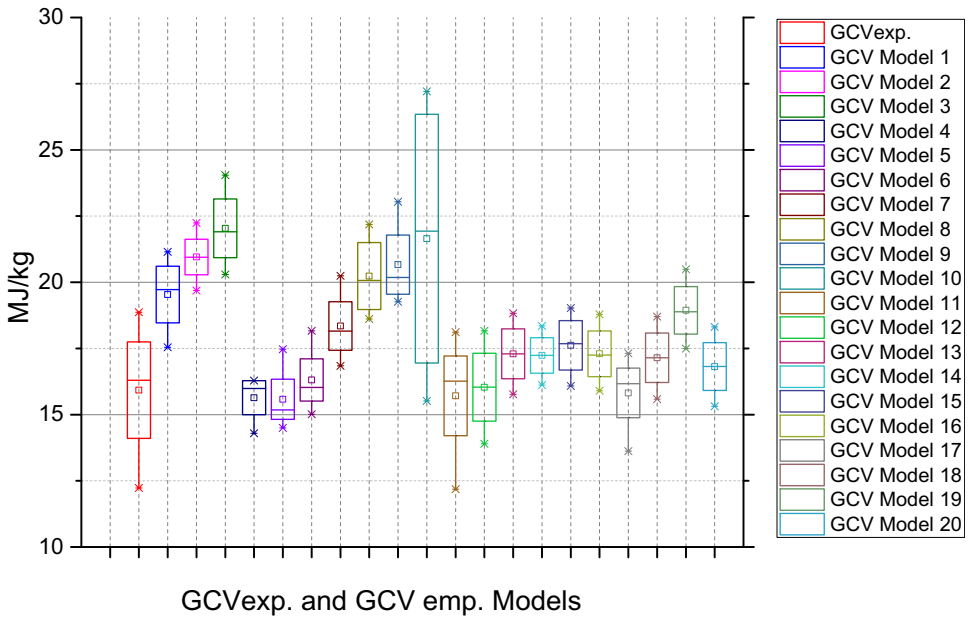

Fig. 1 Box plot of GCV experimental data (average raw MSW) versus GCV empirical prediction models

and consequent heterogeneity of the samples. This can be concluded from the high standard deviations among the repetition of the analysis of the specific blends. PAP30 LIG70 and FDW70 LIG30 revealed the highest GCV among all blends, ΔGCV Group category [30.1–45%]. An explanation for this may be a possible synergistic effect of MSW blends with lignite during combustion. The GCV results of OFMSW sample are in agreement with literature (Matli et al. 2019), regarding several blending proportions of coal with MSW of India. The results of GCV of MSW co-combustion with lignite are comparable to the ones reported in other studies (Vamvuka et al. 2015; Iordanidis et al. 2018).

In addition, in this study, GCV results were used in several new and recently developed tools by the authors of this study, in order to normalize ash production, potential slagging/fouling and maximum potential CO_2, NO and SO_2 emissions. The normalization was carried out by expressing the above-mentioned parameters per produced megajoule, as described in the next paragraphs (see Par. 3.3, 3.6 and 3.11).

3.1.2 Simple regression models of GCV

The estimation of the GCV of blends as a function of the waste content in the blend with lignite (simple regression) can be carried out according to the simple regression equations Eqs. (28) to (31) for every MSW category.

$$\text{FDW: } y = 6.2975\text{x} + 12.337, \quad R^2 = 0.9856 \tag{28}$$

$$\text{GNW: } y = -0.3508x + 12.746, \quad R^2 = 0.1507 \tag{29}$$

$$\text{OFMSW: } y = 4.0578x + 12.329, \quad R^2 = 0.9439 \tag{30}$$

$$\text{PAP: } y = 3.575x + 12.203, \quad R^2 = 0.918 \tag{31}$$

where y is the GCV (MJ/kg) and x is the content of waste in the blend with lignite (x values in the range of 0 to 1.0).

According to the results of the FDW, OFMSW and PAP blends, and by taking into account the characterization of correlation as a function of R according to Evans guide (1996), these blends revealed 'very strong' positive correlation (R: 0.99, 0.97 and 0.96, respectively). GNW blends revealed a weak correlation (R = 0.39) possibly due to high standard deviation among the replications of measurements (see Fig. S2, Supplementary Material).

3.1.3 Experimental results of GCV of MSW versus several empirical models

The comparison of the MSW experimental gross calorific value (average, raw) with 20 empirical models (see Table 1) for predicting GCV is presented in Fig. 1. GCV values calculated by Models 11 and 12 are closer to the experimental results of raw samples. On the other hand, GCV values predicted by models 1, 2, 3, 7, 8, 9, 10 exhibit a high deviation from the experimental results.

A detailed list of the results of the GCV empirical models and the corresponding errors, regarding the experimental data of 17 samples and blends, are presented in Tables 4 and 5, respectively. The GCV errors with regard to experimental values of MSW samples and blends with lignite, as determined by empirical models, are calculated by Eq. (32) where GCV_{Modeli} is the GCV result based on the empirical prediction Model i, i is the number of the

Table 4 GCV of MSW samples and blends with lignite, as determine from empirical models, Eqs. (2)–(21)

Sample ID	Model 1	Model 2	Model 3	Model 4	Model 5	Model 6	Model 7	Model 8	Model 9	Model 10
LIGA	12.56	28.86	17.06	9.85	13.87	14.01	15.00	8.29	8.30	24.97
FDW	21.15	20.88	24.04	16.27	17.47	18.17	20.24	20.81	20.53	27.21
GNW	17.54	22.24	20.29	14.29	14.50	15.01	16.84	18.61	19.83	15.52
OFMSW	19.39	21.01	21.57	15.70	15.21	16.01	18.02	19.33	19.26	25.48
PAP	20.06	19.69	22.24	16.29	15.15	16.05	18.29	22.19	23.04	18.38
FDW70 LIG30	18.58	19.75	18.97	14.42	12.43	13.43	15.50	17.16	16.89	27.09
FDW50 LIG50	17.22	20.98	17.18	14.00	11.25	12.16	14.05	14.60	14.56	25.34
FDW30 LIG70	15.73	23.87	17.25	13.49	12.29	12.98	14.55	12.38	12.15	26.76
GNW70 LIG30	16.38	21.49	17.03	13.95	11.27	12.08	13.91	15.25	15.74	21.19
GNW50 LIG50	15.72	21.90	15.87	13.16	10.37	11.18	12.94	13.34	13.76	21.73
GNW30 LIG70	14.12	24.28	15.42	12.09	10.78	11.43	12.91	11.24	11.44	23.49
OFMSW70 LIG30	17.69	20.42	17.97	14.51	11.75	12.72	14.70	16.41	16.33	25.61
OFMSW50 LIG50	16.36	21.60	16.68	13.71	10.97	11.85	13.67	13.94	13.96	24.83
OFMSW30 LIG70	15.22	22.64	15.52	13.09	10.28	11.13	12.80	11.75	11.58	26.37
PAP70 LIG30	17.96	18.55	17.24	15.32	10.27	11.42	13.64	18.43	19.19	19.12
PAP50 LIG50	16.57	20.95	16.70	13.98	10.69	11.61	13.52	15.75	16.37	20.20
PAP30 LIG70	15.13	24.03	17.00	12.76	12.08	12.65	14.21	12.48	12.75	22.94
Sample ID	Model 11	Model 12	Model 13	Model 14	Model 15	Model 16	Model 17	Model 18	Model 19	Model 20
LIGA	6.35	11.88	13.04	15.06	13.18	13.77	10.20	14.11	15.22	13.89
FDW	18.12	18.17	18.83	18.35	19.02	18.79	17.32	18.70	20.49	18.32
GNW	12.19	13.90	15.77	16.12	16.08	15.91	13.62	15.59	17.50	15.31
OFMSW	16.22	15.61	16.94	17.01	17.28	16.97	16.19	16.84	18.59	16.52
PAP	16.31	16.47	17.65	17.46	18.08	17.53	16.15	17.46	19.18	17.12
FDW70 LIG30	14.87	13.12	15.09	15.71	15.68	15.11	15.36	15.02	16.65	14.76
FDW50 LIG50	12.02	11.92	13.79	15.08	14.42	13.96	13.60	14.14	15.43	13.92
FDW30 LIG70	10.55	12.23	13.67	15.24	14.13	14.05	12.76	14.37	15.51	14.14
GNW70 LIG30	11.17	11.20	13.50	14.70	14.09	13.70	13.08	13.61	15.17	13.41
GNW50 LIG50	9.67	10.50	12.69	14.33	13.34	12.97	12.15	13.10	14.39	12.92
GNW30 LIG70	8.43	10.06	12.16	14.10	12.69	12.61	11.46	12.78	14.02	12.61
OFMSW70 LIG30	13.70	12.20	14.31	15.23	14.92	14.41	14.67	14.35	15.91	14.12
OFMSW50 LIG50	11.26	11.24	13.33	14.72	13.95	13.55	13.16	13.64	15.00	13.44
OFMSW30 LIG70	9.87	10.33	12.42	14.24	13.06	12.76	12.34	12.98	14.17	12.80
PAP70 LIG30	13.26	11.44	13.95	14.82	14.75	13.91	14.32	13.79	15.39	13.58
PAP50 LIG50	11.27	11.08	13.37	14.63	14.04	13.52	13.13	13.52	14.98	13.32
PAP30 LIG70	9.33	11.30	13.31	14.75	13.75	13.67	11.96	13.68	15.14	13.48

Model and $GCV_{experimental}$ is the experimental value of the sample.

$$\text{GCVerror}_{\text{Model}i}(\%) = \frac{(\text{GCV}_{\text{Model}i} - \text{GCV}_{\text{experimental}})}{\text{GCV}_{\text{experimental}}} \cdot 100 \quad (32)$$

For LIGA sample, the best fitted model revealed to be the Model 1 (with error $\leq \pm 1\%$). For FDW sample , the best fitted models revealed to be Model 13, Models 15–16 and Model 18 (with error $\leq \pm 1\%$). For GNW sample the best fitted model was only the Model 11 (error $\leq \pm 1\%$). For OFMSW sample the best fitted model revealed to be Model 20 (error $\leq \pm 1\%$). For PAP sample the best fitted models revealed to be Model 6 and Model 17 (error $\leq \pm 1\%$). For FDW70 LIG30 the best fitted model was Model 19 (error $\leq \pm 1\%$). For FDW50 LIG50 the best fitted model revealed Model 19 (error $\leq \pm 1\%$). For FDW30 LIG70 no model revealed with error $\leq \pm 1\%$. For GNW70 LIG30 the best fitted models revealed Model

Table 5 GCV errors with respect to experimental values of MSW samples and blends with lignite, as determine from empirical models, Eqs. (2)–(21)

Sample ID	Error Model 1	Error Model 2	Error Model 3	Error Model 4	Error Model 5	Error Model 6	Error Model 7	Error Model 8	Error Model 9	Error Model 10
LIGA	− 0.9	127.6	34.5	− 22.3	9.3	10.5	18.3	− 34.6	− 34.6	96.9
FDW	12.1	10.7	27.4	− 13.8	− 7.4	− 3.7	7.3	10.3	8.8	44.2
GNW	43.5	81.9	66.0	16.9	18.6	22.8	37.8	52.2	62.2	26.9
OFMSW	16.7	26.4	29.7	− 5.5	− 8.5	− 3.7	8.4	16.3	15.9	53.3
PAP	25.5	23.2	39.2	1.9	− 5.2	0.4	14.4	38.8	44.2	15.0
FDW70 LIG30	11.7	18.7	14.0	− 13.3	− 25.3	− 19.3	− 6.8	3.2	1.5	62.9
FDW50 LIG50	11.9	36.3	11.6	− 9.1	− 26.9	− 21.0	− 8.7	− 5.1	− 5.4	64.7
FDW30 LIG70	13.6	72.3	24.5	− 2.6	− 11.3	− 6.3	5.0	− 10.7	− 12.3	93.2
GNW70 LIG30	31.4	72.3	36.5	11.8	− 9.6	− 3.1	11.6	22.3	26.2	69.9
GNW50 LIG50	19.9	67.0	21.0	0.4	− 20.9	− 14.7	− 1.3	1.7	4.9	65.7
GNW30 LIG70	14.3	96.5	24.8	− 2.1	− 12.7	− 7.5	4.5	− 9.0	− 7.4	90.1
OFMSW70 LIG30	15.5	33.3	17.3	− 5.3	− 23.3	− 16.9	− 4.0	7.2	6.7	67.2
OFMSW50 LIG50	18.8	56.8	21.1	− 0.5	− 20.4	− 14.0	− 0.8	1.2	1.4	80.2
OFMSW30 LIG70	13.6	69.0	15.8	− 2.3	− 23.3	− 17.0	− 4.5	− 12.3	− 13.6	96.8
PAP70 LIG30	18.7	22.7	14.0	1.3	− 32.1	− 24.5	− 9.8	21.8	26.9	26.4
PAP50 LIG50	20.5	52.4	21.5	1.7	− 22.2	− 15.6	− 1.7	14.6	19.1	46.9
PAP30 LIG70	− 13.4	37.6	− 2.6	− 26.9	− 30.8	− 27.6	− 18.6	− 28.5	− 27.0	31.4

Sample ID	Error Model 11	Error Model 12	Error Model 13	Error Model 14	Error Model 15	Error Model 16	Error Model 17	Error Model 18	Error Model 19	Error Model 20
LIGA	− 50.0	− 6.3	2.8	18.7	3.9	8.6	− 19.6	11.3	20.0	9.5
FDW	− 4.0	− 3.7	− 0.2	− 2.7	0.8	− 0.4	− 8.2	− 0.9	8.6	− 2.9
GNW	− 0.3	13.7	29.0	31.8	31.5	30.1	11.4	27.5	43.1	25.2
OFMSW	− 2.4	− 6.1	1.9	2.4	4.0	2.1	− 2.6	1.3	11.9	− 0.6
PAP	2.1	3.0	10.4	9.3	13.1	9.7	1.0	9.3	20.0	7.1
FDW70 LIG30	− 10.6	− 21.1	− 9.3	− 5.6	− 5.8	− 9.2	− 7.7	− 9.7	0.1	− 11.2
FDW50 LIG50	− 21.9	− 22.6	− 10.4	− 2.1	− 6.3	− 9.3	− 11.6	− 8.1	0.3	− 9.6
FDW30 LIG70	− 23.9	− 11.7	− 1.3	10.0	2.0	1.4	− 7.9	3.7	12.0	2.1
GNW70 LIG30	− 10.4	− 10.2	8.3	17.9	13.0	9.8	4.9	9.2	21.6	7.5
GNW50 LIG50	− 26.3	− 19.9	− 3.2	9.3	1.8	− 1.1	− 7.3	− 0.1	9.8	− 1.5
GNW30 LIG70	− 31.8	− 18.6	− 1.6	14.1	2.7	2.1	− 7.2	3.4	13.4	2.0
OFMSW70 LIG30	− 10.5	− 20.3	− 6.5	− 0.6	− 2.6	− 5.9	− 4.2	− 6.3	3.9	− 7.8
OFMSW50 LIG50	− 18.2	− 18.4	− 3.3	6.9	1.3	− 1.7	− 4.5	− 1.0	8.9	− 2.4
OFMSW30 LIG70	− 26.4	− 22.9	− 7.3	6.3	− 2.5	− 4.8	− 7.9	− 3.1	5.7	− 4.5

Table 5 continued

Sample ID	Error Model 11	Error Model 12	Error Model 13	Error Model 14	Error Model 15	Error Model 16	Error Model 17	Error Model 18	Error Model 19	Error Model 20
PAP70 LIG30	− 12.3	− 24.4	− 7.7	− 2.0	− 2.5	− 8.0	− 5.4	− 8.8	1.8	− 10.2
PAP50 LIG50	− 18.0	− 19.4	− 2.8	6.4	2.1	− 1.6	− 4.5	− 1.6	9.0	− 3.1
PAP30 LIG70	− 46.5	− 35.3	− 23.8	− 15.5	− 21.3	− 21.7	− 31.5	− 21.6	− 13.3	− 22.8

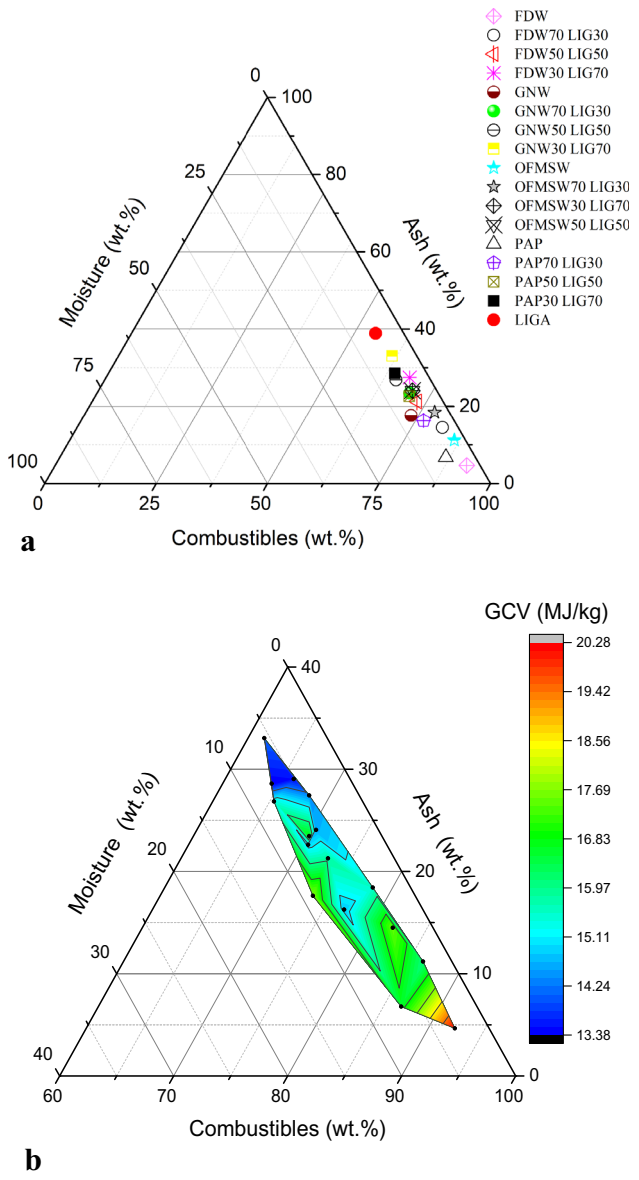

Fig. 2 Results of proximate analysis of the analyzed samples and blends presented in **a** Tanner diagram, **b** the updated Tanner diagram (fourth parameter: GCV), see also Table S1, Supplementary Material

6 and Model 17 (error $\leq \pm 5\%$). For GNW50 LIG50 best fitted models revealed to be Model 4 and Model 18 (error $\leq \pm 1\%$). For GNW30 LIG70 best fitted models revealed to be Model 4, Model 7, Model 13, Model 15–16, Model 18 and Model 20 (error $\leq \pm 5\%$). For OFMSW70 LIG30 the best fitted model was Model 14 (error $\leq \pm 1\%$). The best fitted models for OFMSW50 LIG50 revealed Model 4, Model 7 and Model 18 (error $\leq \pm 1\%$). For OFMSW30 LIG70 best fitted models revealed the Model 4, Model 7, Models 15–16, Model 18 and Model 20 (error $\leq \pm 5\%$). For PAP70 LIG30 best fitted models were Model 4, Model 14–15 and Model 19 (error $\leq \pm 5\%$). For PAP50 LIG50 the best fitted model

Table 6 Results of the environmental footprint indicators (EFI_{sw}) in terms of solid waste production resulting from MSW combustion

Sample ID	Ash production from combustion 100 000 t fuel (t)	%Deviation of sample produced ash from lignite (LIGA) combustion ash (%)	$EFI_{sw,}$ Ash per MJ (kg/MJ)	%Deviation of sample produced ash per MJ from lignite (LIGA) combustion ash (%)
FDW	4660	− 88.02	0.0025	− 91.95
FDW70 LIG30	14,500	− 62.72	0.0087	− 71.60
FDW50 LIG50	21,290	− 45.27	0.0138	− 54.91
FDW30 LIG70	27,440	− 29.46	0.0198	− 35.42
GNW	17,620	− 54.70	0.0144	− 53.04
GNW70 LIG30	23,460	− 39.69	0.0188	− 38.68
GNW50 LIG50	26,850	− 30.98	0.0205	− 33.24
GNW30 LIG70	33,050	− 15.04	0.0267	− 12.84
OFMSW	11,190	− 71.23	0.0067	− 78.05
OFMSW70 LIG30	18,430	− 52.62	0.0120	− 60.79
OFMSW50 LIG50	24,070	− 38.12	0.0175	− 43.02
OFMSW30 LIG70	29,050	− 25.32	0.0217	− 29.33
PAP	6790	− 82.54	0.0042	− 86.15
PAP70 LIG30	16,270	− 58.17	0.0110	− 64.24
PAP50 LIG50	22,610	− 41.88	0.0164	− 46.40
PAP30 LIG70	28,590	− 26.50	0.0225	− 26.68
LIGA	38,900	0.00	0.0307	0.00

revealed Model 4, Model 7, Model 13, Model 15–18 and Model 20 (error $\leq \pm 5\%$). For PAP30 LIG70 the best fitted model was Model 3, with a deviation from experimental results less than 5% (error $\leq \pm 5\%$). More details are presented in Fig. S1 (Supplementary material).

3.2 Proximate analysis via tanner diagrams

The results of proximate analysis of raw MSW samples, their blends with lignite, and lignite (reference sample), are presented in Fig. 2 as triangular diagrams (analytical results are presented in Table S1, Supplementary Material).

All raw MSW samples revealed volatile content more than 70 wt.% in contrast to lignite sample that exhibited a much lower value, namely $\sim$ 43 wt.%. GNW and PAP samples showed the lowest ($\sim$ 72 wt.%) and the highest (82 wt.%) content of volatile matter, respectively, among the raw MSW samples. Volatile content is one of the major factors that influence the stability and reactivity of fuels and the amount of unburned carbon in the ash. Furthermore, volatile content influences the pulverization (grid size) and burner settings. For example, if a fuel with lower volatiles than the respective design value of the burner is used, then, the required fuel thinness needs to be increased in order to have low carbon loss and improved burning efficiency. On the other hand, fuels with high volatiles can be advantageous for ignition because they are easier to ignite. Furthermore, lower NO_x emissions have been reported for fuels with higher volatiles (Miller 2013). These results are in agreement with Gani et al. (2005) who reported that biofuels presented higher volatile matter than coals. In addition, due to the fact that the analyzed samples revealed high volatiles, they can be used in several NO_x reduction techniques, like air staging (or two stage combustion) and reburning.

All raw samples revealed lower ash content (an average $\sim$ 10 wt.%) than the lignite sample ($\sim$ 39 wt.%). Both FDW and PAP revealed low ash content (4.6 wt.% and 6.79 wt.%, respectively). All blends with lignite revealed higher volatile matter than raw lignite, and lower ash content. The results are in agreement with literature (Azam et al. 2020b; Liu et al. 2020). The fuels with low ash content can reduce the quantity of solid wastes resulting from the plant. High concentration of volatiles and low concentration of ash are translated to a high calorific value of a fuel, which means better quality characteristics of a fuel, low solid waste production and low ash related problems in boiler.

Regarding ash content from MSW blends with lignite, values range among the respective values of raw MSW and lignite sample. By increasing the percentage of MSW in the blend with lignite, the volatile content also increases while the ash content decreases. Biomass blends with lignite lead to low NO_x emissions, under excess air condition, unlike coal flame (Hein and Bemtgen 1998). These results are in agreement with the results of GCVs. This tendency is

Table 7 Ultimate analysis (determination of C, H, N, S, and O), and chloride anions (Cl^-) contents of raw MSW, their blends with lignite, and lignite, in different proportions (30 wt.%, 50 wt.%, and 70 wt.%)

Sample ID	C (%)		H (%)		N(%)		S (%)		O (%)[2]	Cl^-	ΔGCV group category
LIGA[1]	35.58	± 0.05	3.73	± 0.06	0.90	± 0.09	< 1.00		19.89	0.02	
FDW	45.70	± 0.48	6.50	± 0.09	1.76	± 0.00	< 0.50		40.88	0.51	[45.1–60%]
GNW	38.83	± 2.19	5.44	± 0.37	1.61	± 0.03	< 0.50		36.00	0.90	[< 0%]
OFMSW	41.59	± 0.54	5.72	± 0.22	1.55	± 0.02	< 0.50		39.46	0.52	[30.1–45%]
PAP	42.97	± 0.02	5.91	± 0.19	0.00	± 0.09	< 0.50		43.84	0.16	[15.1–30%]
MSW_{aver_raw}	42.27	± 0.81	5.89	± 0.22	1.23	± 0.04	< 0.50		40.05	0.52	[15.1–30%]
FDW70 LIG30	37.58	± 0.14	4.82	± 0.07	1.65	± 0.13	0.88	± 0.12	40.57	0.36	[30.1–45%]
FDW50 LIG50	35.64	± 0.27	4.00	± 0.04	1.56	± 0.04	0.66	± 0.13	36.85	0.26	[15.1–30%]
FDW30 LIG70	36.15	± 1.59	3.87	± 0.30	1.20	± 0.09	< 0.50		30.84	0.16	[< 15%]
GNW70 LIG30	34.48	± 0.63	4.16	± 0.19	1.59	± 0.10	0.56	± 0.01	35.76	0.64	[< 0%]
GNW50 LIG50	33.35	± 0.04	3.59	± 0.03	1.41	± 0.03	0.65	± 0.17	34.15	0.46	[< 15%]
GNW30 LIG70	32.65	± 0.34	3.38	± 0.04	1.33	± 0.06	0.73	± 0.06	28.86	0.28	[< 0%]
OFMSW70 LIG30	36.10	± 0.40	4.46	± 0.20	1.69	± 0.10	0.68	± 0.03	38.64	0.37	[15.1–30%]
OFMSW50 LIG50	34.55	± 0.68	3.89	± 0.13	1.37	± 0.07	0.65	± 0.02	35.47	0.27	[< 15%]
OFMSW30 LIG70	33.09	± 0.53	3.39	± 0.08	1.26	± 0.02	0.65	± 0.17	32.56	0.17	[< 15%]
PAP70 LIG30	34.87	± 0.48	4.29	± 0.47	0.88	± 0.18	0.55	± 0.07	43.14	0.11	[15.1–30%]
PAP50 LIG50	34.29	± 1.85	3.99	± 0.03	1.22	± 0.07	0.62	± 0.00	37.28	0.09	[< 15%]
PAP30 LIG70	34.64	± 3.40	4.04	± 0.20	1.51	± 0.12	0.62	± 0.10	30.60	0.06	[30.1–45%]

[1]LIGA sample was analyzed in a previous study by the authors (Vasileiadou et al. 2021a)

[2]Oxygen was calculated by difference. Oxygen was calculated with maximum value of S

Cl^- of MSW blends with lignite were calculated

in agreement with the literature (Hein and Bemtgen 1998). The updated Tanner diagram (Komilis et al. 2014), besides the results of proximate analysis, also takes the GCV into account. Moreover, ash content in the current study is used to normalize the values of slagging, fouling and agglomeration indices (see Par. 3.11).

3.3 Environmental impact of solid wastes production from MSW combustion and their blends with lignite

Table 6 presents the results of the environmental footprint index of the MSW samples (EFI_{sw}) and blends with lignite expressed: (a) as the amount of produced ash per kilogram (kg) of the fuel combustion and (b) as the amount of produced ash per produced megajoule (MJ). The %deviation from the corresponding value of lignite combustion is also included in Table 6.

The results showed that the smallest environmental impact, in terms of ash production, is exhibited by FDW and PAP sample (4660 t ash/100000 t fuel and 6790 t ash/100000 t fuel) whilst the GNW sample showed the highest value (∼ 17,600 t of ash/100000 t of fuel) among the MSW samples and blends, but still, a much lower value than the corresponding value of lignite sample (-54.7%). This comparison is not very representative since it does not take into account the energy produced by the fuel, however, fuels revealed different GCV (MJ/kg). For this reason, an environmental footprint index regarding solid wastes (EFI_{sw}) was developed in order to express the ash production per produced energy (kg ash/MJ).

The results of the EFI_{sw} showed that FDW and PAP sample revealed the lowest environmental impact, 0.0025 t/MJ and 0.0042 t/MJ, respectively, with the corresponding deviation of the produced ash of the lignite combustion to be reduced by 91.95% and 86.15%, respectively. The blends with the highest proportion of waste in blends (70%) revealed the highest (negative) deviation of ash production per MJ compared to the corresponding value of lignite sample.

3.4 Ultimate analysis and ion chromatography results

In Table 7, the results of elemental composition and the results of the chloride content of the raw MSW samples, their blends with lignite, and lignite sample (reference sample) are presented. As it can be seen, the major

elemental constitutes of MSW are carbon, oxygen and hydrogen. All raw samples revealed a higher carbon content (~ 42 w.t%), and a much lower Sulfur content than the lignite sample. The Nitrogen content of raw MSW was higher (~ 1.23 wt.%) than lignite (0.90 wt.%). High N content is not necessarily translated to high NO_x emissions (more details are presented in Par. 3.6).

MSW samples exhibited a higher share of carbon content compared to hydrogen, which increases the energy value (see GCV results). An exception was the PAP sample, in which the oxygen content was higher than the carbon content. The high molar ratio of H/C (> 1.6) of the analyzed samples is responsible for the high volatiles of these fuels.

Regarding the Carbon content of the blends, the FDW blends (with lignite) revealed an average value of approx. 36 wt.% whilst the rest of the blends with lignite revealed a value of about 34 wt.%. The hydrogen content in all blends was approx. 4 wt.%. The nitrogen content in MSW blends with lignite ranges from 0.88 wt.% (PAP70 LIG30) to 1.69 wt.% (OFMSW70 LIG30). The PAP blends with lignite exhibited an average value of about 1.20 wt.% whilst others MSW blends with lignite revealed an average value of about 1.45 wt.%. Regarding Sulfur content, PAP blends (with lignite) revealed the lowest values with an average of approx. 0.60 wt.% whilst FDW blends (with lignite) exhibited the highest values with an average of approx. 0.68 wt.%. In general, samples with high carbon and oxygen concentration (FDW and PAP) exhibited high gross calorific value. Consequently, these blends with lignite revealed a high carbon and oxygen content. Ding et al. (2021) concluded that high oxygen concentration improves co-combustion performance. The results concerning the blends are in agreement with literature findings (Iordanidis et al. 2018; Azam et al. 2020b).

The Chloride content of raw MSW samples was found to be much higher (average value of about 0.52 wt.%) than in the lignite sample (~ 0.02 wt.%). A high amount of chloride content leads to a high number of deposits in surfaces. In the superheater area, the chloride content in ash is strongly corrosive, and creates an additive layer (alkali chlorides, e.g., KCl) that reduces heat transfer. Co-combustion with fuels with sulfur could minimize the corrosion problems which are related to chlorides (Chen et al. 2020). HCl emissions of co-firing are different from conventional coal combustion. HCl emissions are related to combustion temperature, residence time and fuel type. High combustion temperature tends to have a strong effect on HCl emissions. HCl emission during co-combustion also depends on the Cl content of raw fuels and the proportion of fuels included in the solid composite fuel. Mineral additives, such as aluminosilicates can be used in order to reduce HCl emissions (Åmand et al. 2006). Furthermore, regarding the synergistic effect of sulfur in HCl transformation, it is possible to reduce HCl emissions by selecting coal with appropriate sulfur content (Liu et al. 2020). By using co-combustion technology, and fuels that contain sulfur, corrosion could be minimized, as a protective layer can be created which would protect surfaces from Cl corrosion. Moreover, the presence of sulfur in the fuel shifts the melting point of potassium salts (K_2SO_4) to higher temperatures (about 800–1100 °C).

If the S/Cl molar ratio is higher than 4, the fuel is characterized as non-corrosive, whereas if the S/Cl molar ratio is lower than 2, the corrosion of superheaters tubes is unavoidable (Pronobis 2006). MSW blends with lignite exhibited a molar S/Cl ratio higher than 4, namely PAP30 LIG70 (11.96), PAP50 LIG50 (8.09), PAP70 LIG30 (5.37), and OFMSW30 LIG70 (4.37). Fuels with such ratio could be characterized as non-corrosive. Is it is known that the presence of excess sulfur has a beneficial effect on minimizing chlorine corrosion in combustion. For this reason, fewer deposits exists in coal co-combustion (K_2SO_4 is formed instead of KCl) (Leckner 2007). MSW blends with lignite with S/Cl molar ratio lower than 2, namely GNW70 LIG30 (0.97), and GNW50 LIG50 (1.58), could be characterized as corrosive.

Table 8 Empirical chemical formulas of raw MSW and their blends with lignite

Sample ID	Theoretical approximate chemical formula
LIGA[1]	$C_{95}N_2SH_{119}O_{40}$
FDW	$C_{244}N_8SH_{414}O_{164}$
GNW	$C_{207}N_7SH_{346}O_{144}$
OFMSW	$C_{222}N_7SH_{364}O_{158}$
PAP	$C_{229}SH_{376}O_{176}$
$MSW_{average\ raw\ samples}$	$C_{226}N_6SH_{375}O_{161}$
FDW50 LIG50	$C_{144}N_5SH_{192}O_{112}$
FDW30 LIG70	$C_{193}N_6SH_{247}O_{124}$
GNW70 LIG30	$C_{166}N_7SH_{238}O_{129}$
GNW50 LIG50	$C_{136}N_5SH_{174}O_{105}$
GNW30 LIG70	$C_{119}N_4SH_{147}O_{79}$
OFMSW70 LIG30	$C_{141}N_6SH_{207}O_{113}$
OFMSW50 LIG50	$C_{142}N_5SH_{191}O_{109}$
OFMSW30 LIG70	$C_{136}N_4SH_{165}O_{100}$
PAP70 LIG30	$C_{169}N_4SH_{248}O_{157}$
PAP50 LIG50	$C_{147}N_4SH_{203}O_{120}$
PAP30 LIG70	$C_{149}N_6SH_{208}O_{99}$

[1]LIGA empirical chemical formula is from previous study by the authors (Vasileiadou et al. 2021a)

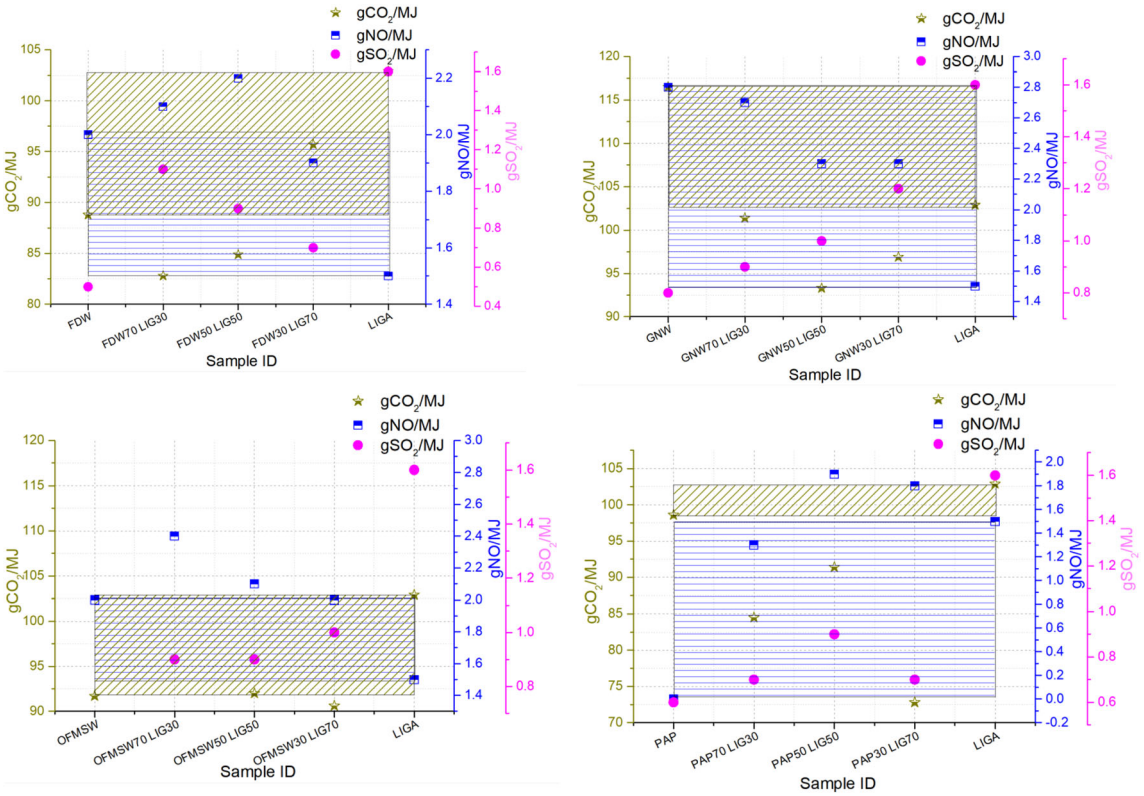

Fig. 3 Results of the maximum potential emission factors of MSW samples and their blends with lignite. LIGA results are from previous study of authors (Vasileiadou et al. 2021c)

3.5 Empirical chemical formulas

Empirical chemical formulas of lignite, MSW raw samples, and their blends with lignite are presented in Table 8. The empirical chemical formula is the simplest number ratio of atoms present in a compound and the most convenient way of expressing the results of the ultimate analysis of a fuel ($C_xN_yS_zH_wO_v$). It is a basic tool for expressing uncharacterized fuels (e.g., wastes, composite fuels, agricultural residues etc.).

The empirical chemical formulas of FDW and GNW found to be $C_{244}N_8SH_{414}O_{164}$ and $C_{207}N_7SH_{346}O_{144}$, respectively, whilst OFMSW was found to be $C_{222}N_7SH_{364}O_{158}$. The empirical chemical formula of PAP was found to be $C_{229}SH_{376}O_{176}$, as it revealed zero nitrogen content. The average MSW theoretical chemical formula is close to the approximate empirical formula calculated by Liwarska-Bizukojc and Ledakowicz (2003). The average empirical chemical formula of MSW blends with lignite was found to be approx. $C_{144}N_5SH_{200}O_{112}$. GNW and OFMSW blends with lignite revealed an average theoretical approximate chemical formula $C_{140}N_5SH_{187}O_{106}$ while FDW blends with lignite revealed $C_{140}N_5SH_{204}O_{109}$ and PAP blends with lignite revealed an average theoretical approximate chemical formula $C_{155}N_5SH_{220}O_{125}$.

3.6 Maximum potential emission factors

The calculated maximum potential emission factors of lignite, raw MSW samples, and MSW blends with lignite are presented in Fig. 3. All samples revealed lower gCO_2/MJ emissions than lignite sample (102.88 gCO_2/MJ). The green waste sample (GNW) was an exception. The average value of MSW was found to be 98.9 gCO_2/MJ. The average value of gNO/MJ emissions of MSW was slightly higher (1.7 gNO/MJ) than lignite sample (1.5 gNO/MJ). The average value of gSO_2/MJ emissions of raw MSW was significantly lower (average 0.6 gSO_2/MJ) than the respective value of lignite (1.6 gSO_2/MJ). More specifically, FDW and OFMSW revealed the lowest values ($\sim$ 0.5 gSO_2/MJ), whilst the GNW sample revealed the highest value (0.8 gSO_2/MJ) of all raw MSW samples. The lowest values of SO_2 emissions of the FDW and OFMSW arise not only from the low S content (< 0.5 wt.%) but also from the fact that these fuels revealed low moisture content ($\sim$ 3 wt.%) and high CaO content (Suksankraisorn et al. 2010). The SO_x and Cl emissions are determined to a large extent by the reactions of gaseous products of combustion but also by the substances that form and react in the ash (Rentizelas 2013). Increased sulfur content is not necessarily translated into increased SO_x emissions as the

occurrence of synergistic effects (reaction with Ca and Mg, forming $CaSO_4$, $MgSO_4$) -natural desulfurization- can result into negligible sulfur emissions. The lower sulfur content of some of MSW could decrease SO_x emissions compared to lignite. These emission factors are in agreement with the volatile matter of the samples.

Regarding MSW blends with lignite, PAP blends with lignite revealed the lowest value of maximum potential CO_2, NO and SO_2 emissions, with average values of 82.9 gCO_2/MJ, 1.67 gNO/MJ, and 0.77 gSO_2/MJ, respectively, whilst the GNW blends with lignite revealed the highest average values and were equal to 97.2 gCO_2/MJ, 2.43 gNO/MJ, and 1.03 gSO_2/MJ, respectively. In general, most of the nitrogen which is present in a biomass fuel is transformed to NH radicals (as NH_3) during combustion. Ammonia reduces NO to molecular nitrogen and as a result reduces the NOx emissions during co-combustion (Hein and Bemtgen 1998). Biomass co-combustion with coal, in a coal fluidized bed boiler could reduce NO_2 and N_2O (Demirbaş 2003). Similar results about reduced emission in MSW co-combustion with lignite due to synergy effect has been reported (Suksankraisorn et al. 2010). The burner configuration for the biomass co-combustion with coal is a crucial factor in the combustion process and has a great impact on the formation of NOx (if the fuel added by the central gun, enters the sub-stoichiometric inner recirculation zone, this results in low NOx emission), and it has been reported that fuels with high nitrogen content should be injected into the center of PF unit (pulverized combustion) (Hein and Bemtgen 1998). Furthermore, alkali components found in biomass residues could affect the SO_x removal. The lower sulfur and the transformation in the form of solid alkali sulfates, are retained in the ash and lead to reduced SO_2 emissions (Pedersen et al. 1997). Several technologies (e.g., biomass co-firing desulfurization-BCD) could reduce SO_x emissions by 60–65% compared to initial levels. Dong et al. (2002) reported that although it is known that in a bubbling fluidized bed, as the temperature is increased, the formation rate of SO_2 is also increased, during co-combustion of MSW and coal in circulating fluidized bed (CFB), SO_2 emissions remain the same by increasing temperature. The tendency of emission factors per produced megajoule (gNO/MJ) in every raw MSW and their blends with lignite, appeared different from the tendency shown in the nitrogen content.

In FDW and their blends with lignite, regarding nitrogen content (see the results of ultimate analysis), as the percentage of FDW in blend increases, the nitrogen content also increases. However, the respective nitrogen oxide emissions (expressed per produced MJ), do not follow the same trend, since the blends exhibit higher GCV values (the raw FDW exhibits the highest GVA among all samples) and possibly some synergy effects might take place.

Table 9 Combustion characteristics of lignite, raw MSW and their blends

Sample ID	T_i (°C)	T_b (°C)	T_{max} (°C)	R_{max} (%/min)	t_b (min)	Total weight loss (%)	ΔGCV group category
LIGA[1]	237	927	888	1.640	66.77	63.43	
FDW	181	960	281	4.332	75.47	96.99	[45.1–60%]
GNW	228	857	296	4.181	60.79	85.10	[< 0%]
OFMSW	157	968	291	4.707	78.38	91.19	[30.1–45%]
PAP	235	807	334	5.600	55.22	94.37	[15.1–30%]
$MSW_{average\_raw}$	200	899	300	4.705	67.46	91.91	[15.1–30%]
FDW70 LIG30	232	938	307	3.721	68.45	86.99	[30.1–45%]
FDW50 LIG50	232	978	310	2.729	72.39	79.82	[15.1–30%]
FDW30 LIG70	216	980	312	1.845	74.05	73.48	[< 15%]
GNW70 LIG30	224	915	268	2.477	66.98	78.42	[< 0%]
GNW50 LIG50	226	917	271	2.005	66.92	74.08	[< 15%]
GNW30 LIG70	228	919	274	1.539	66.93	70.66	[< 0%]
OFMSW70 LIG30	199	930	289	3.104	70.85	82.64	[15.1–30%]
OFMSW50 LIG50	200	932	291	2.553	70.85	77.65	[< 15%]
OFMSW30 LIG70	245	934	294	1.805	66.77	72.15	[< 15%]
PAP70 LIG30	246	860	343	4.087	59.18	85.11	[15.1–30%]
PAP50 LIG50	248	901	299	3.239	63.10	79.20	[< 15%]
PAP30 LIG70	251	940	301	2.270	66.73	72.27	[30.1–45%]

[1]LIGA Results from a previous study by the authors (Vasileiadou et al. 2021a)

3.7 Thermogravimetric and derivative thermogravimetric (TG/DTG) analysis

The combustion characteristics resulting from TG/DTG analysis, of the raw MSW samples, MSW blends with lignite, and lignite sample (reference sample) are presented in Table 9. All raw MSW samples revealed significantly lower T_{max} and significantly higher R_{max} than LIGA, and this is translated to higher reactivity (Miller 2013). MSW exhibited much higher total weight loss (average ~ 92 wt.%) than lignite (~ 63 wt.%). The above-mentioned results are in agreement with the results of proximate analysis regarding the ash content. High reaction rate was observed in wastes with high oxygen concentration. These results are in agreement with literature (Muthuraman et al. 2010). PAP sample revealed the highest reaction rate whilst GNW revealed the lowest reaction rate among MSW samples. These results are in agreement with the oxygen content measured in this study.

OFMSW blends with lignite ignite earlier (average approx. 214 °C), followed by GNW blends and FWD blends with lignite (average approx. 227 °C), followed by PAP blends with lignite (average approx. 249 °C). Easy ignition is based on the volatile matter, the ash content and the H/C ratio of a fuel (Vamvuka et al. 2015) as well as the oxygen content (Muthuraman et al. 2010). The combustion of PAP blends with lignite occurs at shorter time (an average of about 63 min) whilst in the FDW blends with lignite it occurs at longer time (an average of about 72 min). PAP blends with lignite revealed the highest maximum temperature at which there is the highest rate of weight loss (314 °C, 3.2%/min) whilst GNW blends with lignite revealed the lowest maximum temperature (271 °C, 2.0%/min).

The TG and DTG profiles of the analyzed raw MSW samples are illustrated in Fig. 4. A typical peak of the samples with the maximum weight loss is observed between 250 and 350 °C (see DTG curves). It can be seen that the maximum peak temperature and the maximum rate of weight loss of FDW, GNW and OFMSW samples, were lower than in the PAP sample, which means that these samples can be combusted at lower temperature and consequently, could exhibit lower NOx emissions. As can be seen, all raw MSW revealed the highest peak temperature with the highest rate of weight loss. All blends with a percentage of 30 wt.% MSW revealed the lowest peak temperature, whilst those with 70 wt.% MSW content in blend with lignite, revealed the highest. The maximum combustion rate increased when the MSW proportion was increased in the blend with lignite. In most of blends, the more the MSW blend ratio is increased, the more the maximum temperature is decreased. Furthermore, as the biomass content is increased in the blends with lignite, in the DTG profile of the fuel, the peak height (R_{max}) is also increased. These results are in agreement with literature for other lignite/biomass mixtures (energy crop named arundo donax with lignite, cotton residue with lignite and refused derived fuel with lignite) studied by Vamvuka et al. (2020).

3.8 Comparison between experimental and calculated (theoretical) DTG profiles of MSW blends with lignite—synergistic effect

In order to study the potential existence of synergistic effect of the MSW co-combustion with lignite, the theoretical profiles of derivative thermogravimetric analysis DTG curves were calculated and compared with the respective experimental DTG curves. The theoretical DTG curve and the experimental DTG curve of every MSW blend with lignite are illustrated in Fig. 5.

A synergistic effect was observed in the food waste (FDW) blends, specifically in the stage after moisture removal (> 200 °C) as the FDW blends showed the maximum mass loss (R_{max}) at a higher maximum temperature (T_{max}) in the experimental DTG curves, from corresponding temperature in the theoretical DTG curves (especially in blend with 70 wt.% FDW) due to the interaction of the two fuels that take part in the mixture (waste and lignite) during co-combustion. The release of heat during the combustion of the volatiles took place at a higher maximum temperature compared to the corresponding temperature of the theoretical DTG curves. Synergistic effects were also observed in FDW blends with lignite, at the last stage of combustion (after 800 °C) since two small peaks were found in the experimental DTG curves, where they initiate to form at lower temperatures, instead of one peak that exists in the corresponding theoretical DTG curve. In green waste blends, co-combustion with lignite might be slightly inhibited (lower R_{max}, %/min). A similar trend was also observed in the literature during coal co-combustion with sewage sludge (Prabhakaran 2020). In PAP blends with lignite, no strong synergistic effects emerged as the theoretical DTG curves are almost identical to the experimental DTG curves.

3.9 Activation energy determination and Arrhenius plot—kinetic modeling

Kinetic modeling parameters (activation energy, pre-exponential factor and correlation factor) were determined from the TG/DTG data and are presented in Table 10. The data of every analyzed sample, of Stage III, the stage in which the combustion initiates, were fitted to an Arrhenius plot. Arrhenius plots (1/T versus logK) of raw MSW and their blends with lignite are illustrated in Fig. 6. Stage III is different for the lignite sample. Kinetic values of all other

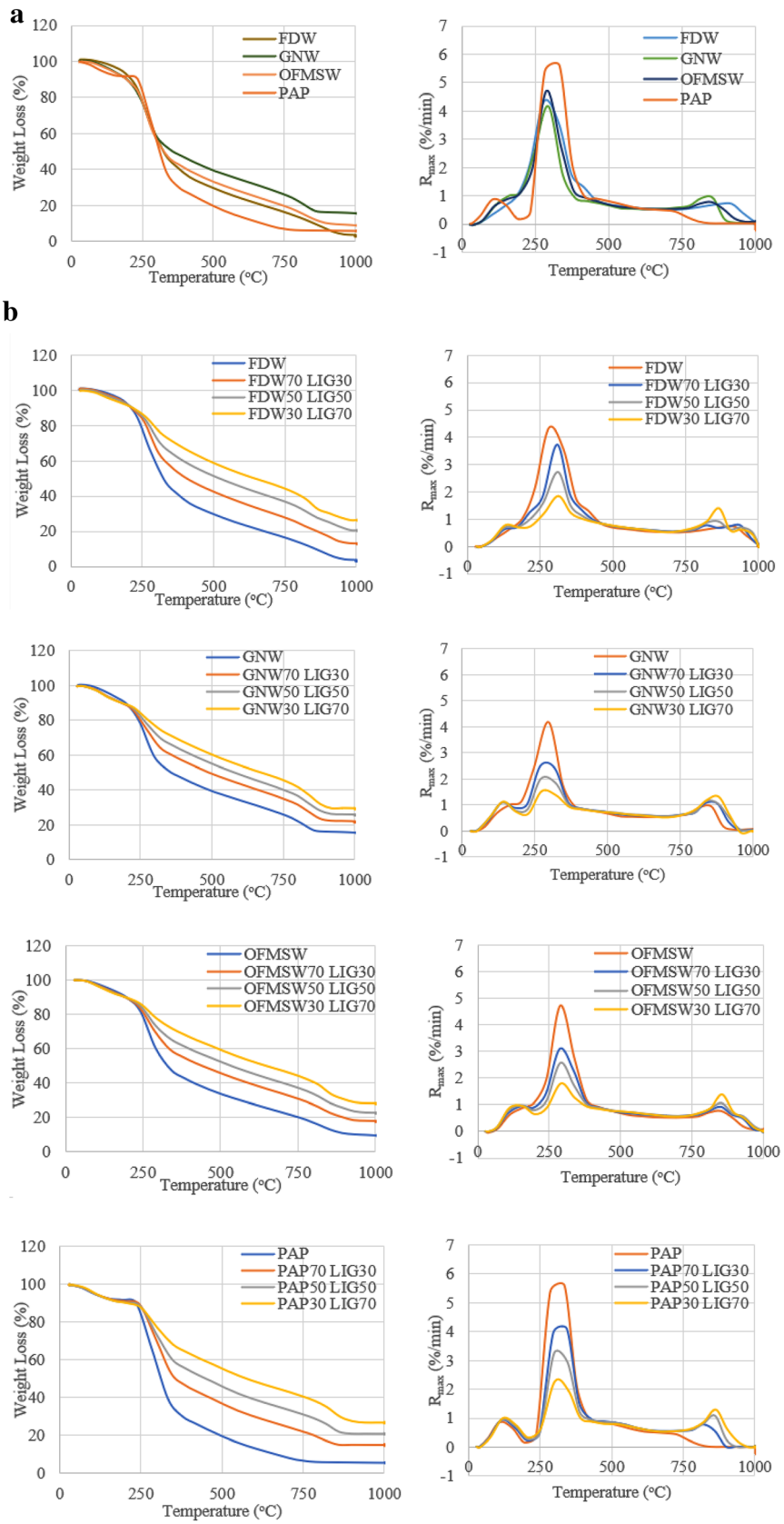

Fig. 4 Left: TG profiles, Right: DTG profiles: a. Raw MSW, b. Raw MSW samples compared to their blends with lignite (heating rate: 10 °C/min, flow rate: 3.5 l/min)

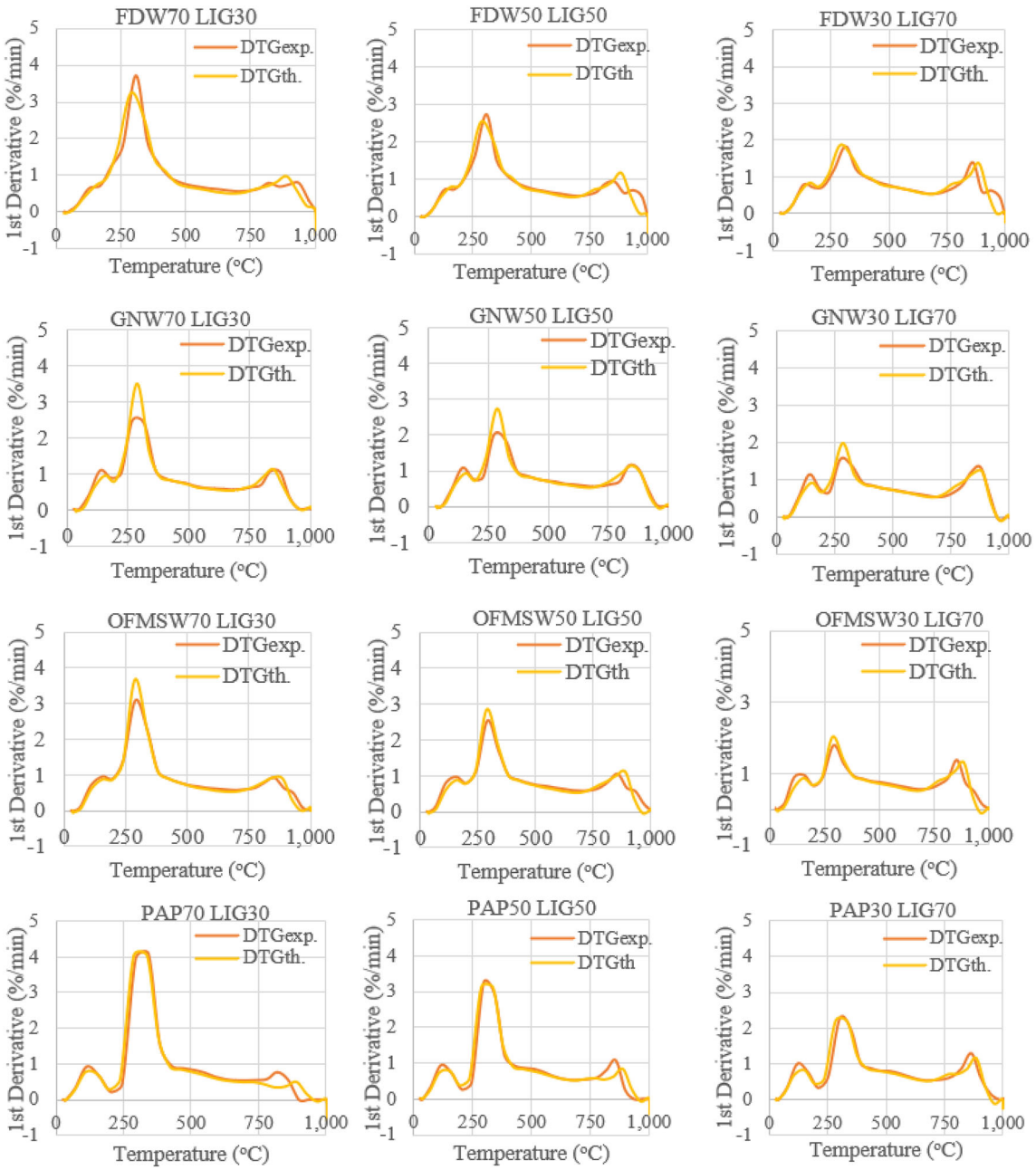

Fig. 5 Comparison between experimental and calculated DTG curves of MSW blends with lignite

analyzed samples (and blends) refer to Stage III. More details can be found in previous work of the authors (Vasileiadou et al. 2021a). GNW revealed the lowest activation energy among all samples (~ 40 kJ/mol), followed by FDW (~ 43 MJ/mol) and OFMSW (~ 46 kJ/mol) that is translated to higher reaction rate. PAP sample revealed higher activation energy (~ 85 kJ/mol) than lignite (~ 71 kJ/mol). Pre-exponential factor of raw MSW samples that is also related to the reaction rate of the sample, was found to be higher than lignite. PAP sample revealed the higher pro-exponential factor which means that the molecules of this sample collide more often than the other analyzed raw samples. The results are in agreement with Azam et al. (2019) that studied coal and MSW of Pakistan and found that MSW revealed lower activation energy than coal.

FDW blends with lignite revealed the lowest activation energy among all blends with an average value of around 25 kJ/mol followed by OFMSW and GNW blends (average value around 34 kJ/mol), whilst the PAP blends with lignite revealed the highest activation energy, with an average value of about 67 kJ/mol. The minimum value of

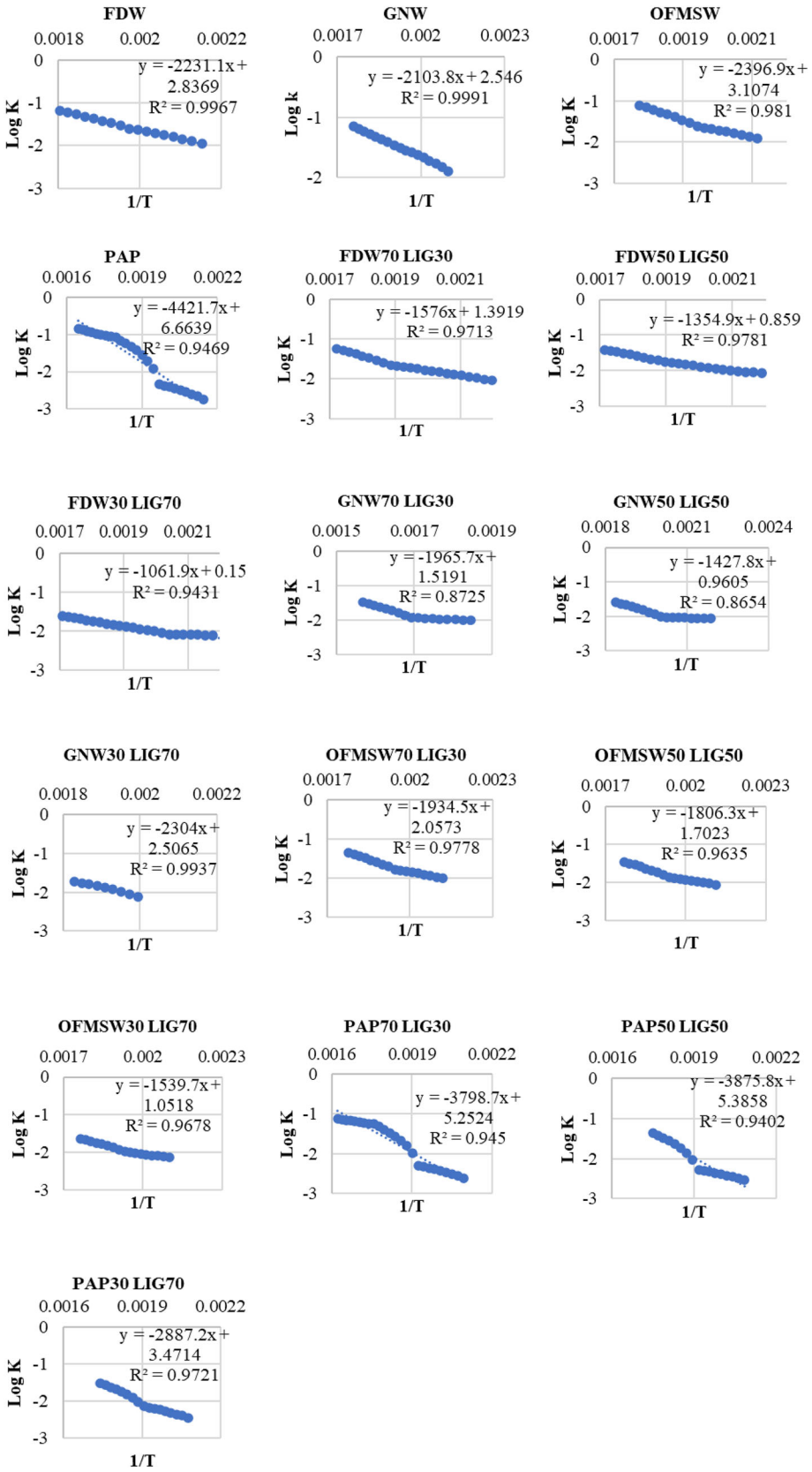

Fig. 6 Arrhenius plots of the analyzed samples and blends

Table 10 Kinetic parameters of lignite, raw MSW and their blends

Sample ID	T range (°C)		*a*	*b*	R^2	*E* (kJ/mol)	*A* (s^{-1})
	From	To					
LIGA[1]	695	889	− 435.81	− 1.31	0.9686	70.79	8.17E-04
FDW	192	281	− 2231	2.837	0.9967	42.72	11.45
GNW	204	296	− 2104	2.546	0.9991	40.28	5.859
OFMSW	199	291	− 2397	3.107	0.9810	45.89	21.34
PAP	193	334	− 4422	6.664	0.9469	84.66	76,876
$MSW_{average\_raw}$	197	301	− 2789	3.789	0.9809	53.39	19,228.7
FDW70 LIG30	171	307	− 1576	1.392	0.9713	30.18	0.411
FDW50 LIG50	174	310	− 1355	0.859	0.9781	25.94	0.12
FDW30 LIG70	176	312	− 1062	0.15	0.9431	20.33	0.024
GNW70 LIG30	182	268	− 1569	1.344	0.8919	30.05	0.368
GNW50 LIG50	184	271	− 1428	0.961	0.8654	27.34	0.152
GNW30 LIG70	228	274	− 2304	2.507	0.9937	44.12	5.35
OFMSW70 LIG30	199	289	− 1934	2.057	0.9778	37.04	1.902
OFMSW50 LIG50	200	291	− 1806	1.702	0.9635	34.59	0.84
OFMSW30 LIG70	202	294	− 1540	1.052	0.9678	29.48	0.188
PAP70 LIG30	204	343	− 3799	5.252	0.9450	72.73	2980
PAP50 LIG50	207	299	− 3876	5.386	0.9402	74.21	4052
PAP30 LIG70	209	301	− 2887	3.471	0.9721	55.28	49.35

[1]LIGA result from previous study of authors (Vasileiadou et al. 2021a)

activation energy of every MSW category, was exhibited by FDW30 LIG70, GNW50 LIG50, OFMSW30 LIG70 and PAP30 LIG70 which may be an optimal option for every MSW category. Fuels with low activation energy have high reaction rates. This is in agreement with R_{max} of the analyzed samples.

In FDW blends and OFMSW blends with lignite, the pre-exponential factor increased by increasing the proportion of the waste in the blend with lignite. In GNW blends and PAP blends this was not observed. Furthermore, a possible synergistic effect could exist since most of MSW blends with lignite do not fall within the area defined by the raw fuels (see hatched area, see Fig. S1, Supplementary Material). All FDW and OFMSW blends with lignite revealed lower activation energy than the raw samples. This can also be observed, for blends with 70 wt.% GNW, 50 wt.% GNW and 30 wt.% PAP.

3.10 Enthalpy change, Gibbs free energy and entropy change determination via Thermodynamic analysis

TG/DTG data with 10 °C/min were used to evaluate the thermodynamic parameters at the same degradation stage as for the kinetic parameters. The thermodynamic parameters elucidate the reaction of MSW decomposition during combustion, as shown in Table 11. Enthalpy change is the energy that is needed to break the reagent bonds. Samples with high activation energy, yielded high ΔH_α. PAP and LIGA revealed the highest enthalpy change among all raw samples (approx. 85 and 71 kJ/mol respectively) which is translated to higher energy needed in order to separate the reagent bonds. PAP sample showed the highest difference in Gibbs free energy, 210 kJ/mol whilst the samples FDW and GNW showed the lowest value (approx. 150 kJ/mol). Lower value of ΔG_α is translated to lower amount of energy production (Chong et al. 2019). All raw samples showed similar entropy change, ΔS_α. Enthalpy change of the FDW and OFMSW blends with lignite revealed lower values than raw samples (not within the region of raw samples). Similar tendency is observed for blends with 30 wt.% PAP, 30 wt.% GNW and 70 wt.% GNW. This may occur due to the synergistic effect of MSW blends with lignite. Regarding the Gibbs free energy change, all blends presented lower values than raw samples. Regarding entropy change, all blends reveal similar values.

3.11 Ash characterization using SEM–EDS analysis and slagging/fouling indices

Table 12 presents the results of chemical ash composition of MSW ashes. Si, Ca, K, and P are the major ash forming elements occurring in biomass combustion whilst Si, Ca, Mg and K are the main components in lignite ash. The results are in agreement with literature studies (Loo and Koppejan 2008; Iordanidis et al. 2020).

Table 11 Thermodynamic parameters of MSW and their blends with lignite

Sample ID	T range (°C)		T_m (K)	ΔH_α (kJmol^{-1})	ΔG_α (kJmol^{-1})	$\Delta S\alpha$ (kJmol^{-1} K^{-1})
	From	To				
LIGA	695	889	1162	61.13	296.99	− 0.20
FDW	192	281	554	38.11	149.84	− 0.20
GNW	204	296	569	35.55	150.89	− 0.20
OFMSW	199	291	564	41.21	155.38	− 0.20
PAP	193	334	607	79.62	209.08	− 0.21
$MSW_{average\_raw}$	197	301	574	48.62	166.30	− 0.20
FDW70 LIG30	171	307	581	25.35	141.11	− 0.20
FDW50 LIG50	174	310	583	21.09	135.87	− 0.20
FDW30 LIG70	176	312	585	15.47	128.37	− 0.19
GNW70 LIG30	182	268	542	25.54	130.81	− 0.19
GNW50 LIG50	184	271	544	22.82	127.45	− 0.19
GNW30 LIG70	228	274	547	39.57	144.35	− 0.19
OFMSW70 LIG30	199	289	562	32.37	143.61	− 0.20
OFMSW50 LIG50	200	291	565	29.89	140.46	− 0.20
OFMSW30 LIG70	202	294	567	24.77	133.93	− 0.19
PAP70 LIG30	204	343	617	67.61	195.73	− 0.21
PAP50 LIG50	207	299	572	69.46	182.67	− 0.20
PAP30 LIG70	209	301	574	50.51	162.43	− 0.19

Table 12 Elemental analysis of MSW ashes, blends and lignite (as a reference ash sample)

Sample ID	SiO_2 (%)	CaO (%)	K_2O (%)	P_2O_5 (%)	Al_2O_3 (%)	MgO (%)	Fe_2O_3 (%)	SO_3 (%)	Na_2O (%)	TiO_2 (%)
LIGA	20.49	37.2	13.60	3.44	3.03	17.48	0.00	4.05	0.00	0.00
FDW	13.58	30.39	5.28	25.48	3.91	11.31	2.14	1.25	8.09	0.00
GNW	14.92	59.67	0.40	1.83	8.65	4.23	1.30	4.38	3.67	0.00
OFMSW	14.97	52.03	13.83	3.85	2.95	3.33	1.80	0.58	4.53	0.00
PAP	20.74	16.65	18.83	6.50	5.80	2.79	6.95	2.73	0.61	0.00
FDW70 LIG30*	19.54	36.77	12.14	8.5	3.32	16.61	0.48	3.26	1.82	0.00
FDW50 LIG50*	20.2	37.31	13	5.93	3.2	17.21	0.23	3.7	0.89	0.00
FDW30 LIG70*	21.02	38.46	13.77	4.71	3.21	17.92	0.11	4.01	0.41	0.00
GNW70 LIG30*	18.03	49.87	6.98	2.67	6.05	10.92	0.69	4.32	1.93	0.00
GNW50 LIG50*	19.74	46.52	9.98	3.09	5.03	14.05	0.43	4.37	1.21	0.00
GNW30 LIG70*	19.27	40.19	11.27	3.12	3.88	15.08	0.21	4.03	0.59	0.00
OFMSW70 LIG30*	19.33	45.66	14.49	3.81	3.17	12.49	0.77	2.81	1.92	0.00
OFMSW50 LIG50*	20.03	42.15	14.21	3.67	3.13	14.9	0.42	3.4	1.05	0.00
OFMSW30 LIG70*	20.93	40.88	14.35	3.67	3.18	16.77	0.21	3.86	0.52	0.00
PAP70 LIG30*	22.01	32.3	17.03	5.21	4.12	13.36	2.03	4.28	0.18	0.00
PAP50 LIG50*	21.39	34.89	15.44	4.37	3.61	15.46	1.04	4.19	0.09	0.00
PAP30 LIG70*	21.3	36.8	14.73	3.94	3.36	16.85	0.5	4.19	0.04	0.00

*Blends were calculated by the authors

FDW revealed the lowest SiO_2 value (13.58 wt.%) among all raw MSW ashes, whilst PAP revealed the highest value, about 20 wt.%, a similar value to lignite sample. Silica content in ash is a major indicator of slagging. Ohman et al. (2004) reported that a range between 20 and 25 wt.% is crucial.

Regarding CaO concentration, GNW and OFMSW revealed high concentration (more than 52 wt.%) whilst

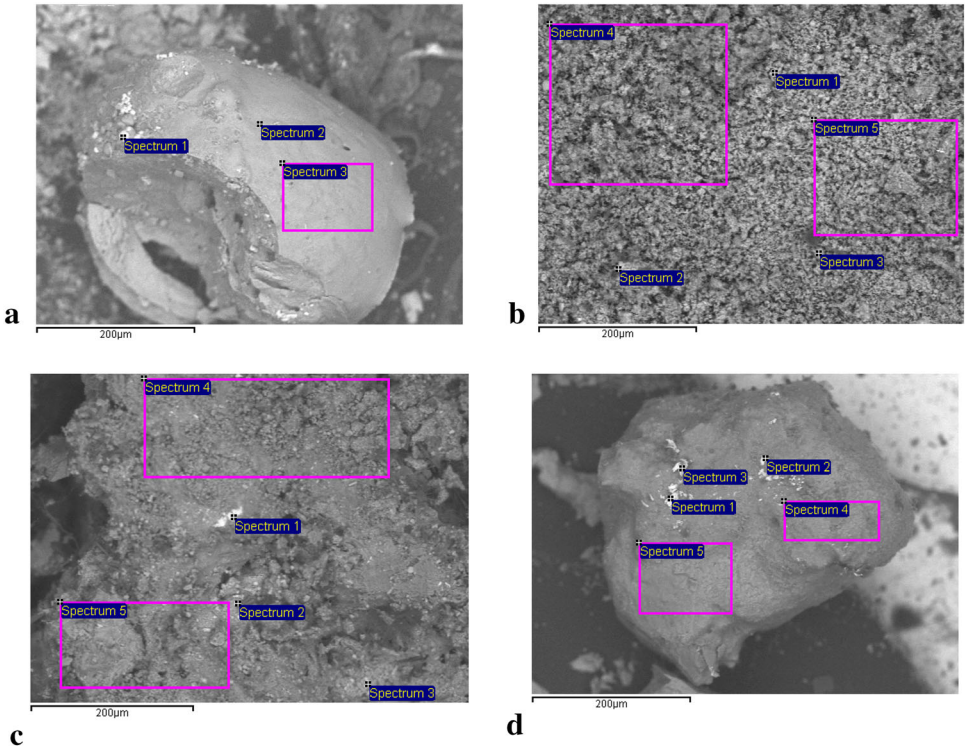

Fig. 7 Results SEM spectrums: **a** FDW, **b** GNW, **c** OFMSW and **d** PAP sample

PAP ash sample revealed a value lower than 17 wt.%. If in the ash fuel there is more than 50 wt.% of CaO or SiO_2 and at the same time there is more than 15 wt.% of K_2O, then the ash of the fuel creates agglomerations and deposits (García et al. 2015). The analyzed ashes do not present the above combination. The high CaO content could also assist in natural desulfurization in the blends and further reduce SO_x emissions. Regarding MgO, the MSW ash raw samples revealed an average value of 5.42 wt.% whilst the lignite sample revealed more than 17 wt.%. In general, as Ca and Mg content is increased, the melting temperature increases and the slagging potential decreases. Most of the biomass fuels revealed high Nitrogen, chlorine content and variety of ash forming metals (e.g., K).

One way to eliminate these problems is to combine fuels in co-combustion with specific characteristics (e.g., high CaO, MgO, S etc.), or/and use additives (e.g., kaolin, calcite), in order to increase the melting temperature of the fuel ash and reduce the slagging/fouling and agglomeration phenomena in the combustion plant.

PAP revealed the highest concentration of K_2O ($\sim$ 19 wt.%) among all ashes, while GNW revealed very low K_2O concentration (0.40 wt.%). Regarding P_2O_3 concentration, FDW revealed the highest amount of phosphorus oxide among all ashes.

In general, the elements of the chemical analysis should not be analyzed individually but in various combinations with each other to study the tendency to form slag, deposits, agglomerations, etc. Therefore, various slagging, fouling and agglomeration indicators have been developed (Pronobis 2005; Vasileiadou et al. 2021c).

In Fig. 7, SEM images are presented along with the points/areas that were used to obtain the spectra of the analyzed ash samples. The ash morphology of the MSW samples is different in each sample. For example, the ash particles of the green waste sample were found to be smaller and uniform with each other in contrast to the ash of the food waste sample, where the ash particles were not all similar to each other.

The results of slagging and fouling indices and the modified ash indices are illustrated in Tables 13 and 14, respectively. The ranges for the modified indices are presented in previous work of authors (Vasileiadou et al. 2022). These modified indices take into account literature ash indices, that is the chemical composition of ash but also the gross calorific value results as well as the ash content from the proximate results. For the above-mentioned reasons, the modified ash indices lead to a more objective evaluation of the slagging and fouling tendency of the solid fuels. More detailed information can be found in previous recent work of the authors (Vasileiadou et al. 2022).

The characterization of the modified Cl index of FDW and OFMSW was 'low' and 'high', respectively, due to high energy content and due to low ash content. SiO_2 index in GNW sample changed from 'low' to 'medium' (in the modified index) due to the effect of GCV (low GCV, about

Table 13 Results of the slagging and fouling indices

Sample ID	Cl		SiO_2		B/A		BAI		Rs		Fu		Sr	
LIGA	0.02	L	20.49	M	3.05	EH	0.00	H	3.05	EH	41.47	H	27.26	H
FDW	0.51	EH	13.58	L	4.73	EH	0.09	H	2.42	H	63.21	H	23.65	H
GNW	0.90	EH	14.92	L	3.02	EH	0.32		1.51	M	12.28	M	18.62	H
OFMSW	0.52	EH	14.97	L	4.43	EH	0.10	H	2.22	H	81.37	H	20.75	H
PAP	0.16	L	20.74	M	1.97	EH	0.36		0.99	M	38.33	M	44.01	H
FDW70 LIG30	0.36	H	19.54	L	3.34	EH	0.03	H	2.94	EH	46.61	H	26.62	H
FDW50 LIG50	0.26	M	20.2	M	3.19	EH	0.02	H	2.10	H	44.26	H	26.95	H
FDW30 LIG70	0.16	L	21.02	M	3.11	EH	0.01	H	1.56	M	44.11	H	27.12	H
GNW70 LIG30	0.64	EH	18.03	L	3.03	EH	0.08	H	1.70	M	27.03	M	22.68	H
GNW50 LIG50	0.46	H	19.74	L	3.04	EH	0.04	H	1.98	M	34.01	M	24.45	H
GNW30 LIG70	0.28	M	19.27	L	3.04	EH	0.02	H	2.22	H	36.10	M	25.78	H
OFMSW70 LIG30	0.37	H	19.33	L	3.52	EH	0.05	H	2.39	H	57.72	H	24.70	H
OFMSW50 LIG50	0.27	M	20.03	M	3.30	EH	0.03	H	2.14	H	50.34	H	25.85	H
OFMSW30 LIG70	0.17	L	20.93	M	3.17	EH	0.01	H	2.06	H	47.12	H	26.56	H
PAP70 LIG30	0.11	L	22.01	M	2.68	EH	0.12	H	1.48	M	46.18	H	31.58	H
PAP50 LIG50	0.09	L	21.39	M	2.85	EH	0.07	H	1.77	M	44.29	H	29.39	H
PAP30 LIG70	0.06	L	21.3	M	2.95	EH	0.03	H	1.83	M	43.64	H	28.23	H

where *EH* extremely high, *H* high, *M* medium, *L* low

12 MJ/kg) and the ash content (about 18 wt.%) of the sample. LIGA changed from 'medium' (SiO_2 index) to 'high' tendency (modified SiO_2 index). B/A index in all samples (except PAP and FDW) remained 'extremely high' in the modified B/A index. The average value of BAI index of MSW is 0.20. BAI index with values lower than 0.15, suggest high slagging tendency (Bapat et al. 1997). In the modified BAI index all ashes (except GNW) revealed a high tendency. Regarding the Rs index, two of the four raw MSW ash samples (PAP and GNW) revealed a medium tendency for slagging whilst OFMSW and FDW revealed a high tendency. The average value of MSW is 1.79 (medium tendency). In modified Rs index, GNW revealed a 'high' tendency, while FDW and PAP revealed 'low' tendency. Since the values of the ash samples in Fu index are higher than 40 (except GNW), they are related to 'high' fouling inclination whilst GNW is related to 'medium' fouling tendency. The modified Fu index of PAP changed into 'medium' fouling tendency. Since all ash samples revealed Sr values lower than 65, this indicates high slagging potential. The only sample that revealed different characterization in the modified Sr, compared to Sr index, is LIGA.

According to the total Ash Quality Index (tAQI) (Vasileiadou et al. 2022), ashes of PAP and FDW are characterized by lower fouling and slagging tendency than GNW and OFMSW. Regarding blends, FDW70 LIG30 and PAP70 LIG30 revealed to have lower fouling and slagging tendency than other blends.

3.12 Case studies (scenarios) of energy recovery of wastes—waste to energy (WtE)

In Table 15, the results of various scenarios (case studies) on energy production from municipal solid waste combustion are presented. More specifically, for these case studies, food wastes, green wastes and paper/ cardboard wastes that represent 54.6% of the municipal solid wastes were taken into account. The variables that were used are presented in Sect. 2.

For *Greece,* according to *Scenario I,* potential energy production from the MSW combustion, ranges from 1.14E + 10 MJ/year (cs 4, combust only 30% of the produced specific MSW) to 3.79E + 10 MJ/year (cs 1, combust 100% of the produced specific MSW). In other words, by using 43.9% of MSW, 36% of food wastes and green wastes, and 18.6% paper/cardboard waste, and not taking into account the 10.6% which is composted (World Bank 2018), and knowing that the primary energy production in Greece, in year 2017 was 7.5 Mtoe, according to Scenario I, 3.6% to 12.1% of the energy demand could be covered by the combustion of the MSW. According to *Scenario II* (projections for the year 2030), the energy production in Greece, that could be produced from the MSW combustion ranges from 7.02E + 09 MJ/year to 2.34E + 10 MJ/year covering 2.0% and 6.6%, respectively, of the 8.48 Mtoe of Greece primary energy production (demand). According to *Scenario III* (projections for the year 2030), *Greece* could cover from 1.3 to 4.4% of the required 10.2 Mtoe (Greece primary energy production, forecast for the year 2060),

Table 14 Results of the modified slagging and fouling indices of ash samples

Sample ID	Modif. Cl (kg/GJ)		Modif. SiO_2 (kg/GJ)		Modif. B/A (kg/GJ)		Modif. BAI (kg/GJ)		Modif. Rs (kg/GJ)		Modif. Fu (kg/GJ)		Modif. Sr (kg/GJ)	
LIGA	0.000	L	6.29	H	93.55	EH	0.00	H	0.94	EH	12.72	H	8.36	L
FDW	0.013	L	0.34	L	11.93	H	0.40	H	0.06	L	5.23	H	0.78	H
GNW	0.130	EH	2.15	M	43.46	EH	4.61		0.22	H	1.77	M	2.68	H
OFMSW	0.035	H	1.01	L	29.84	EH	0.66	H	0.15	M	5.48	H	1.40	H
PAP	0.007	L	0.88	L	8.55	M	1.52		0.04	L	2.18	M	1.97	H
FDW70 LIG30	0.031	H	1.70	L	29.09	EH	0.30	H	0.26	H	4.06	H	2.32	H
FDW50 LIG50	0.036	H	2.79	H	44.08	EH	0.23	H	0.29	EH	6.12	H	3.73	H
FDW30 LIG70	0.032	H	4.16	H	61.64	EH	0.15	H	0.31	EH	8.74	H	5.37	H
GNW70 LIG30	0.120	EH	3.39	H	57.08	EH	1.46	H	0.32	EH	5.09	H	4.27	H
GNW50 LIG50	0.094	EH	4.04	H	62.24	EH	0.79	H	0.40	EH	6.97	H	5.01	H
GNW30 LIG70	0.075	EH	5.15	H	81.39	EH	0.47	H	0.59	EH	9.65	H	6.89	M
OFMSW70 LIG30	0.045	H	2.33	M	42.31	EH	0.56	H	0.29	EH	6.94	H	2.97	H
OFMSW50 LIG50	0.047	H	3.50	H	57.66	EH	0.48	H	0.37	EH	8.80	H	4.52	H
OFMSW30 LIG70	0.037	H	4.54	H	68.70	EH	0.31	H	0.45	EH	10.22	H	5.76	H
PAP70 LIG30	0.012	L	2.41	M	29.44	EH	1.29	H	0.16	M	5.07	H	3.46	H
PAP50 LIG50	0.015	L	3.52	H	46.89	EH	1.10	H	0.29	EH	7.28	H	4.83	H
PAP30 LIG70	0.013	L	4.79	H	66.46	EH	0.76	H	0.41	EH	9.82	H	6.35	H

where *EH* extremely high, *H* high, *M* medium, *L* low

using only 30% of the MSW (FDW, GNW, and PAP) and 100% of the produced MSW, respectively.

For *Europe,* according to *Scenario I* (using data from the year 2017), energy production from MSW combustion could range from 4.62E + 11 MJ/year, covering 1.5% of 758.2 Mtoe of EU primary energy production (using only 30% of MSW) to 1.54E + 12 MJ/year (using 100% of the specific MSW). According to *Scenario II,* potential energy cover will be reduced and ranges from 0.9% of 856.8 Mtoe of EU primary energy production (cs 4, using 30% of the produced MSW) to 3.0% (cs 1, using 100% of the produced MSW) of 856.8 Mtoe of EU primary energy production which correspond to energy demands for the year 2030. Forecast for energy cover in Europe for year 2060 showed that burning MSW could produce from 2.57E + 11 MJ/year (cs 4, using 30% of the produced MSW) to 8.56E + 11 MJ/year (cs 1, using 100% of the produced MSW).

4 Conclusions

In this work, several MSWs were evaluated for their potential to be used as a primary fuel in combustion or/and as auxiliary fuel in co-combustion with lignite. A comprehensive assessment of combustion and other characteristics (energy content, proximate analysis, ultimate analysis, ion chromatography, thermogravimetric and differential thermogravimetric analysis), kinetic modeling and thermodynamic analysis along with ash elemental analysis were performed. Maximum potential emissions and the empirical chemical formulas were calculated from the ultimate analysis and were expressed per produced MJ. The environmental impact regarding solid waste production of the combustion, was also expressed per produced MJ. Ash quality was evaluated by determining its composition by SEM-EDS and by calculating various slagging/fouling indices including the proposed ones in literature and also the new modified indices developed previously by the authors of the current study. Furthermore, twenty empirical GCV models were used in order to find the best fitted models for the experimental results. Moreover, several scenarios (case studies) were developed in order to evaluate the potential cover of energy demands in Greece, and Europe from the combustion of MSW. Several modified fouling/slagging indices that were developed in a previous study by the authors were used for the assessment of several MSW categories and their blends with lignite in several proportions. CO_2, NO and SO_2 emission factors of the analyzed samples and MSW blends with lignite were expressed per produced energy.

The results of this study showed:

- The environmental footprint index, the emission factors and the modified slagging indices expressed per

Table 15 Scenarios (Case studies) of waste-to-energy (WtE)

Cases studies (cs)		Scenario I (year 2017)	Scenario II (forecast for 2030)	Scenario III (forecast for 2060)
Case study 1	100% of MSW of this study (:54.6% of MSW–10.7% compost) for energy production, in Greece, in Mtoe/year	0.91 Mtoe/year [3.79E + 10 MJ/year] (12.1% of 7.5 Mtoe of Greece primary energy production)	0.56 Mtoe/year [2.34E + 10 MJ/year] (6.6% of 8.48 Mtoe of Greece primary energy production)	0.45 Mtoe/year [1.86E + 10 MJ/year] (4.4% of 10.2 Mtoe of Greece primary energy production)
	100% of MSW of this study (:54.6% of MSW–10.7% compost) for energy production, in EU, Mtoe/year	36.80 Mtoe/year [1.54E + 12 MJ/year] (4.9% of 758.2 Mtoe of EU primary energy production)	25.67 Mtoe/year [1.07E + 12 MJ/year] (3.0% of 856.8 Mtoe of EU primary energy production)	20.45 Mtoe/year [8.56E + 11 MJ/year] (2.0% of 1031.2 Mtoe of EU primary energy production)
Case study 2	70% of MSW of this study (:54.6% of MSW–10.7% compost) for energy production, in Greece, Mtoe/year	0.63 Mtoe/year [2.65E + 10 MJ/year] (8.5% of 7.5 Mtoe of Greece primary energy production)	0.39 Mtoe/year [1.64E + 10 MJ/year] (4.6% of 8.48 Mtoe of Greece primary energy production)	0.31 Mtoe/year [1.31E + 10 MJ/year] (3.1% of 10.2 Mtoe of Greece primary energy production)
	70% of MSW of this study (:54.6% of MSW–10.7% compost) for energy production, in EU, Mtoe/year	25.76 Mtoe/year [1.08E + 12 MJ/year] (3.4% of 758.2 Mtoe of EU primary energy production)	17.97 Mtoe/year [7.52E + 11 MJ/year] (2.1% of 856.8 Mtoe of EU primary energy production)	14.32 Mtoe/year [5.99E + 11 MJ/year] (1.4% of 1031.2 Mtoe of EU primary energy production)
Case study 3	50% of MSW of this study (:54.6% of MSW–10.7% compost) for energy production, in Greece, Mtoe/year	0.45 Mtoe/year [1.90E + 10 MJ/year] (6.0% of 7.5 Mtoe of Greece primary energy production)	0.28 Mtoe/year [1.17E + 10 MJ/year] (3.3% of 8.48 Mtoe of Greece primary energy production)	0.22Mtoe/year [9.32E + 09 MJ/year] (2.2% of 10.2 Mtoe of Greece primary energy production)
	50% of MSW of this study (:54.6% of MSW–10.7% compost) for energy production, in EU, Mtoe/year	18.40 Mtoe/year [7.70E + 11 MJ/year] (2.4% of 758.2 Mtoe of EU primary energy production)	12.83 Mtoe/year [5.37E + 11 MJ/year] (1.5% of 856.8 Mtoe of EU primary energy production)	10.23 Mtoe/year [4.28E + 11 MJ/year] (1.0% of 1031.2 Mtoe of EU primary energy production)
Case study 4	30% of MSW of this study (:54.6% of MSW–10.7% compost) for energy production, in Greece Mtoe/year	0.27 Mtoe/year [1.14E + 10 MJ/year] (3.6% of 7.5 Mtoe of Greece primary energy production)	0.17 Mtoe/year [7.02E + 09 MJ/year] (2.0% of 8.48 Mtoe of Greece primary energy production)	0.13 Mtoe/year [5.59E + 09 MJ/year] (1.3% of 10.2 Mtoe of Greece primary energy production)
	30% of MSW of this study (:54.6% of MSW–10.7% compost) for energy production, in EU, Mtoe/year	11.04 Mtoe/year [4.62E + 11 MJ/year] (1.5% of 758.2 Mtoe of EU primary energy production)	7.70 Mtoe/year [3.22E + 11 MJ/year] (0.9% of 856.8 Mtoe of EU primary energy production)	6.14 Mtoe/year [2.57E + 11 MJ/year] (0.6% of 1031.2 Mtoe of EU primary energy production)

produced energy, that is, by taking into account not only the chemical composition but also GCV and ash content of the fuel, could be useful tools for characterization and categorization alternative solid biofuels (e.g., agricultural wastes, composite fuels, industrial wastes origin from biomass etc.).

- Raw MSW samples revealed much better combustion characteristics, e.g., higher calorific values, higher volatiles, lower ash, lower sulfur emissions, etc., but a slightly higher nitrogen maximum emission potential than lignite.
- Nitrogen oxide emissions do not necessarily follow the trend in fuel's nitrogen content and might be low despite the high nitrogen content due to high GCV. This can be revealed if the emissions are expressed per MJ of produced energy instead of kg of fuel.
- The percentage of MSW in the blend with lignite positively affects the combustion characteristics.

- Synergistic effects seem to occur in the MSW co-combustion with lignite since most of the blends revealed lower activation energy than raw samples which means that the blends ignite more easily in combustion. The existence of synergy effect is further supported by the shifting of experimental DTC curves compared to calculated (theoretical) DTG curves of blends.
- The smallest environmental impact, in terms of ash production, was exhibited by FDW (0.0025 t/MJ) and PAP sample (0.0042 t/MJ) with the corresponding deviation of the produced ash of the lignite combustion to be reduced by 91.95% and 86.15%, respectively, whilst the GNW sample showed the highest value (0.0144 t/MJ) among the MSW samples and blends, but it still exhibited a much lower value than the corresponding value of lignite sample (-53.04%).
- Raw MSW samples, in terms of their reactivity during combustion, can be classified in the following order: PAP > OFMSW > FDW > GNW.
- The Chloride content of MSW raw samples was found to be considerably higher than the one of lignite sample.
- The amount of produced MSW in Greece and Europe could contribute to cover up to 12% and 5%, respectively, of the primary energy production.

The results of this study suggest that the MSW combustion and MSW co-combustion with lignite could be a promising alternative renewable energy source, and thus, it can be considered as an environmentally friendly energy source that could cover a considerable portion of the world's energy demands. Additional benefits of co-combustion may also include the reduction of fossil fuels and the development of a local biofuel market. However, the increased nitrogen and chlorine content of MSW may increase capital cost, due to the demand of equipment/process for denitrogenation and/or reducing related emissions.

Supplementary Information The online version contains supplementary material available at https://doi.org/10.1007/s40974-023-00271-y.

Acknowledgements This research is co-financed by Greece and the European Union (European Social Fund- ESF) through the Operational Programme «Human Resources Development, Education and Lifelong Learning» in the context of the project "Strengthening Human Resources Research Potential via Doctorate Research – 2nd Cycle" (MIS-5000432), implemented by the State Scholarships Foundation (IKΥ).

Author contributions AV contributed to the conceptualization, investigation, methodology, data curation, validation, formal analysis, writing—original draft, writing—review and editing, visualization, review and editing; SZ was involved in the supervision; AD assisted in the review and editing; all authors have read and agreed to the published version of the manuscript.

Funding Open access funding provided by HEAL-Link Greece.

Declarations

Conflict of interest The authors have no conflicts of interest.

Ethical standards This article does not contain any studies involving human or animal subjects.

References

Abu-Qudais Md, Abu-Qdais HA (2000) Energy content of municipal solid waste in Jordan and its potential utilization. Energy Conv Manage 41:983–991. https://doi.org/10.1016/S0196-8904(99)00155-7

Al-Qayim K, Nimmo W, Hughe KJ, Pourkashanian M (2019) Effect of oxy-fuel combustion on ash deposition of pulverized wood pellets. Biofuel Res J 6:927–936. https://doi.org/10.18331/brj2019.6.1.4

Alrobaian AA (2020) Improving waste incineration CHP plant efficiency by waste heat recovery for feedwater preheating process: energy, exergy, and economic (3E) analysis. J Braz Soc Mech Sci Eng 42:403. https://doi.org/10.1007/s40430-020-02460-w

Åmand L-E, Leckner B, Eskilsson D, Tullin C (2006) Deposits on heat transfer tubes during co-combustion of biofuels and sewage sludge. Fuel 85:1313–1322. https://doi.org/10.1016/j.fuel.2006.01.001

ASTM International (2013) ASTM D5865 - 13 Standard Test Method for Gross Calorific Value of Coal and Coke. ASTM International, West Conshohocken, PA. https://www.astm.org/

ASTM International (2015) ASTM D 7582–15 Standard Test Methods for Proximate Analysis of Coal and Coke by Macro Thermogravimetric Analysis. ASTM International, West Conshohocken. PA. https://www.astm.org/

Azam M, Jahromy SS, Raza W, Jordan C, Harasek M, Winter F (2019) Comparison of the combustion characteristics and kinetic study of coal, municipal solid waste, and refuse-derived fuel: Model-fitting methods. Energy Sci Eng 7:2646–2657. https://doi.org/10.1002/ese3.450

Azam M, Ashraf A, Jahromy SS, Raza W, Khalid H, Raza N, Winter F (2020a) Isoconversional nonisothermal kinetic analysis of municipal solid waste, refuse-derived fuel, and coal. Energy Sci Eng 8:3728–3739. https://doi.org/10.1002/ese3.778

Azam M, Jahromy SS, Raza W, Raza N, Lee SS, Kim K-H, Winter F (2020b) Status, characterization, and potential utilization of municipal solid waste as renewable energy source: Lahore case

study in Pakistan. Environ Int 134:105291. https://doi.org/10.1016/j.envint.2019.105291
Bapat DW, Kulkarni SV, Bhandarkar VP (1997) Design and operating experience on fluidized bed boiler burning biomass fuels with high alkali ash. American Society of Mechanical Engineers
Boumanchar I, Chhiti Y, Mhamdi Alaoui FE, Sahibed-dine A, Bentiss F, Jama C, Bensitel M (2018) Municipal solid waste higher heating value prediction from ultimate analysis using multiple regression and genetic programming techniques. Waste Manag Res 37:578–589. https://doi.org/10.1177/0734242X18816797Sun
Bourtsalas AC, Huang Q, Zhang H, Themelis NJ (2020) Energy recovery in China from solid wastes by the moving grate and circulating fluidized bed technologies. Waste Dispos Sustain Energy 2:27–36. https://doi.org/10.1007/s42768-019-00026-8
Chen L, Liao Y, Xia Y, Ma X (2020) Combustion characteristics of co-combusted municipal solid wastes and sewage sludge. Energy Sour Part A Recov Util Environ Eff. https://doi.org/10.1080/15567036.2020.1739175
Chong CT, Mong GR, Ng J-H, Chong WWF, Ani FN, Lam SS, Ong HC (2019) Pyrolysis characteristics and kinetic studies of horse manure using thermogravimetric analysis. Energy Convers Manage 180:1260–1267. https://doi.org/10.1016/j.enconman.2018.11.071
Cumming JW (1984) Reactivity assessment of coals via a weighted mean activation energy. Fuel 63:1436–1440. https://doi.org/10.1016/0016-2361(84)90353-3
Demirbaş A (2003) Sustainable cofiring of biomass with coal. Energy Convers Manage 44:1465–1479. https://doi.org/10.1016/S0196-8904(02)00144-9
Ding G, He B, Yao H, Cao Y, Su L, Duan Z (2021) Co-combustion behaviors of municipal solid waste and low-rank coal semi-coke in air or oxygen/carbon dioxide atmospheres. J Therm Anal Calorim 143:619–635. https://doi.org/10.1007/s10973-019-09170-z
Dong C, Jin B, Zhong Z, Lan J (2002) Tests on co-firing of municipal solid waste and coal in a circulating fluidized bed. Energy Convers Manage 43:2189–2199. https://doi.org/10.1016/S0196-8904(01)00157-1
Escamilla-García PE, Camarillo-López RH, Carrasco-Hernández R, Fernández-Rodríguez E, Legal-Hernández JM (2020) Technical and economic analysis of energy generation from waste incineration in Mexico. Energy Strategy Rev 31:100542. https://doi.org/10.1016/j.esr.2020.100542
Eurostat, (2019) Energy, transport and environment statistics. European Union. https://doi.org/10.2785/499987
Eurostat (2020) Population. Eurostat. https://ec.europa.eu/
Evans JD (1996) Straightforward statistics for the behavioral sciences. Brooks/Cole Publishing
Gani A, Morishita K, Nishikawa K, Naruse I (2005) Characteristics of co-combustion of low-rank coal with biomass. Energy Fuels 19:1652–1659. https://doi.org/10.1021/ef049728h
García R, Pizarro C, Álvarez A, Lavín AG, Bueno JL (2015) Study of biomass combustion wastes. Fuel 148:152–159. https://doi.org/10.1016/j.fuel.2015.01.079
Gidarakos E, Havas G, Ntzamilis P (2006) Municipal solid waste composition determination supporting the integrated solid waste management system in the island of Crete. Waste Manage 26:668–679. https://doi.org/10.1016/j.wasman.2005.07.018
Gu W, Liu D, Wang C (2021) Energy recovery potential from incineration using municipal solid waste based on multi-scenario analysis in Beijing. Environ Sci Pollut Res 28:27119–27131. https://doi.org/10.1007/s11356-021-12478-9
Hein KRG, Bemtgen JM (1998) EU clean coal technology—co-combustion of coal and biomass. Fuel Process Technol 54:159–169. https://doi.org/10.1016/S0378-3820(97)00067-2
Hupa M, Karlström O, Vainio E (2017) Biomass combustion technology development – It is all about chemical details. Proc Combust Inst 36:113–134. https://doi.org/10.1016/j.proci.2016.06.152
Iordanidis A, Asvesta A, Vasileiadou A (2018) Combustion behaviour of different types of solid wastes and their blends with lignite. Therm Sci 22:1077–1088. https://doi.org/10.2298/tsci170704219i
Iordanidis A, Asvesta A, Kapageridis I, Vasileiadou A, Koios K, Oikonomidis S, Kantiranis N (2020) A comprehensive analytical characterization of Greek lignite Bottom ash samples. Therm Sci 25:1879–1888. https://doi.org/10.2298/TSCI200606299I
Jiménez L, González F (1991) Study of the physical and chemical properties of lignocellulosic residues with a view to the production of fuels. Fuel 70:947–950. https://doi.org/10.1016/0016-2361(91)90049-G
Kathiravale S, Muhd Yunus MN, Sopian K, Samsuddin AH, Rahman RA (2003) Modeling the heating value of Municipal Solid Waste. Fuel 82:1119–1125. https://doi.org/10.1016/S0016-2361(03)00009-7
Komilis D, Evangelou A, Giannakis G, Lymperis C (2012) Revisiting the elemental composition and the calorific value of the organic fraction of municipal solid wastes. Waste Manag 32:372–381. https://doi.org/10.1016/j.wasman.2011.10.034
Komilis D, Kissas K, Symeonidis A (2014) Effect of organic matter and moisture on the calorific value of solid wastes: An update of the Tanner diagram. Waste Manage 34:249–255. https://doi.org/10.1016/j.wasman.2013.09.023
Leckner B (2007) Co-combustion a summary of technology. AGS Energy Pathways Flagship Program. ISBN 978-91-633-0295-4
Li Z, Lu Q, Na Y (2004) N2O and NO emissions from co-firing MSW with coals in pilot scale CFBC. Fuel Process Technol 85:1539–1549. https://doi.org/10.1016/j.fuproc.2003.10.025
Liu H, Wang Y, Zhao S, Hu H, Cao C, Li A, Yu Y, Yao H (2020) Review on the current status of the co-combustion technology of organic solid waste (OSW) and coal in China. Energy Fuels 34:15448–15487. https://doi.org/10.1021/acs.energyfuels.0c02177
Liu J-I, Paode RD, Holsen TM (1996) Modeling the energy content of municipal solid waste using multiple regression analysis. J Air Waste Manag Assoc 46:650–656. https://doi.org/10.1080/10473289.1996.10467499
Liwarska-Bizukojc E, Ledakowicz S (2003) Stoichiometry of the AEROBIC BIODEGRADATION OF THE ORGANIC FRACTION OF MUNICIPAL SOLID WAste (MSW). Biodegradation 14:51–56. https://doi.org/10.1023/A:1023538123655
Loo Sv, Koppejan J (2008) The handbook of biomass combustion and co-firing. Earthscan, UK, ISBN 978-1-84407-249-1
Matli C, Challa B, Kadaverugu R (2019) Co-firing municipal solid waste with coal - A case study of Warangal City, India. Nat Environ Pollut Technol 18:237–245
Medina-Mijangos R, De Andrés A, Guerrero-Garcia-Rojas H, Seguí-Amórtegui L (2021) A methodology for the technical-economic analysis of municipal solid waste systems based on social cost-benefit analysis with a valuation of externalities. Environ Sci Pollut Res 28:18807–18825. https://doi.org/10.1007/s11356-020-09606-2
Miles TR, Miles J, T R, Baxter LL, Bryers RW, Jenkins BM, Oden LL (1995) Alkali deposits found in biomass power plants: A preliminary investigation of their extent and nature. Volume 1. NREL/TP-433-8142-Vol.1; SAND-96-8225-Vol.1; Other: ON: DE96007897; TRN: AHC29614%%16 United States https://doi.org/10.2172/251288 Other: ON: DE96007897; TRN:

AHC29614%%16 OSTI as DE96007897 NREL English, ; National Renewable Energy Lab., Golden, CO (United States); Miles (Thomas R.), Portland, OR (United States); Sandia National Labs., Livermore, CA (United States); Foster Wheeler Development Corp., Livingston, NJ (United States); California Univ., Davis, CA (United States); Bureau of Mines, Albany, OR (United States). Albany Research Center

Miller B (2013) 3 - Fuel considerations and burner design for ultra-supercritical power plants. In: Zhang D (ed) Ultra-supercritical coal power plants. Woodhead Publishing, pp 57–80

Mushtaq J, Dar AQ, Ahsan N (2020) Physio-chemical characterization of municipal solid waste and its management in high-altitude urban areas of North-Western Himalayas. Waste Disposal Sustain Energy 2:151–160. https://doi.org/10.1007/s42768-020-00040-1

Muthuraman M, Namioka T, Yoshikawa K (2010) A comparison of co-combustion characteristics of coal with wood and hydrothermally treated municipal solid waste. Biores Technol 101:2477–2482. https://doi.org/10.1016/j.biortech.2009.11.060

OECD (2018) Global material resources outlook to 2060. Econ Drivers Environ Conseq. https://doi.org/10.1787/9789264307452-en

Öhman M, Nordin A, Hedman H, Jirjis R (2004) Reasons for slagging during stemwood pellet combustion and some measures for prevention. Biomass Bioenerg 27:597–605. https://doi.org/10.1016/j.biombioe.2003.08.017

Parikh J, Channiwala SA, Ghosal GK (2005) A correlation for calculating HHV from proximate analysis of solid fuels. Fuel 84:487–494. https://doi.org/10.1016/j.fuel.2004.10.010

Pedersen LS, Morgan DJ, Van De Kamp WL, Christensen J, Jespersen P, Dam-Johansen K (1997) Effects on SOx and NOx emissions by co-firing straw and pulverized coal. Energy Fuels 11:439–446. https://doi.org/10.1021/ef960110k

Peng X, Ma X, Xu Z (2015) Thermogravimetric analysis of co-combustion between microalgae and textile dyeing sludge. Biores Technol 180:288–295. https://doi.org/10.1016/j.biortech.2015.01.023

Perera SMHD, Wickramasinghe C, Samarasiri BKT, Narayana M (2021) Modeling of thermochemical conversion of waste biomass – a comprehensive review. Biofuel Res J 8:1481–1528. https://doi.org/10.18331/brj2021.8.4.3

Prabhakaran SPS, Viraj VJ (2020) Energy conservation – a novel approach of co-combustion of paint sludge and Australian lignite by principal component analysis, response surface methodology and artificial neural network modeling. Environ Technol Innov 20:101061. https://doi.org/10.1016/j.eti.2020.10106

Pronobis M (2005) Evaluation of the influence of biomass co-combustion on boiler furnace slagging by means of fusibility correlations. Biomass Bioenerg 28:375–383. https://doi.org/10.1016/j.biombioe.2004.11.003

Pronobis M (2006) The influence of biomass co-combustion on boiler fouling and efficiency. Fuel 85:474–480. https://doi.org/10.1016/j.fuel.2005.08.015

Rentizelas AA (2013) 2 - Biomass supply chains. In: Rosendahl L (ed), Biomass combustion science, technology and engineering. Woodhead Publishing, pp 9–35. https://doi.org/10.1533/9780857097439.1.9

Sahu P, Prabu V (2022) Techno-economic analysis on oxy-fuel based steam turbine power system using municipal solid waste and coals with ultrasonicator sulfur removal. Waste Disposal Sustain Energy 4:131–147. https://doi.org/10.1007/s42768-022-00100-8

Sarigiannis DA, Handakas EJ, Karakitsios SP, Gotti A (2021) Life cycle assessment of municipal waste management options. Environ Res 193:110307. https://doi.org/10.1016/j.envres.2020.110307

Sheng C, Azevedo JLT (2005) Estimating the higher heating value of biomass fuels from basic analysis data. Biomass Bioenerg 28:499–507. https://doi.org/10.1016/j.biombioe.2004.11.008

Suksankraisorn K, Patumsawad S, Fungtammasan B (2010) Co-firing of Thai lignite and municipal solid waste (MSW) in a fluidised bed: Effect of MSW moisture content. Appl Therm Eng 30:2693–2697. https://doi.org/10.1016/j.applthermaleng.2010.07.020

Tian L, Lin K, Zhao Y, Zhao C, Huang Q, Zhou T (2022) Combustion performance of fine screenings from municipal solid waste: Thermo-kinetic investigation and deep learning modeling via TG-FTIR. Energy 243:122783. https://doi.org/10.1016/j.energy.2021.122783

Tillman DA (1978) Wood as an energy resource. Academic Press

Toscano G, Riva G, Foppa Pedretti E, Duca D (2013) Effect of the carbon oxidation state of biomass compounds on the relationship between GCV and carbon content. Biomass Bioenerg 48:231–238. https://doi.org/10.1016/j.biombioe.2012.11.002

Vamvuka D, Sfakiotakis S, Saxioni S (2015) Evaluation of urban wastes as promising co-fuels for energy production – A TG/MS study. Fuel 147:170–183. https://doi.org/10.1016/j.fuel.2015.01.070

Vamvuka D, Loukakou E, Sfakiotakis S, Petrakis E (2020) The impact of a combined pre-treatment on the combustion performance of various biomass wastes and their blends with lignite. Thermochim Acta 688:178599. https://doi.org/10.1016/j.tca.2020.178599

Vasileiadou A, Zoras S, Dimoudi A, Iordanidis A, Evagelopoulos V (2020) Compost of biodegradable municipal solid waste as a fuel in lignite co-combustion. Environ Res Eng Manag 76:60–67. https://doi.org/10.5755/j01.erem.76.4.24168

Vasileiadou A, Zoras S, Iordanidis A (2021a) Bioenergy production from olive oil mill solid wastes and their blends with lignite: thermal characterization, kinetics, thermodynamic analysis, and several scenarios for sustainable practices. Biomass Convers Biorefin. https://doi.org/10.1007/s13399-021-01518-6

Vasileiadou A, Zoras S, Iordanidis A (2021b) Biofuel potential of compost-like output from municipal solid waste: multiple analyses of its seasonal variation and blends with lignite. Energy 236:121457. https://doi.org/10.1016/j.energy.2021.121457

Vasileiadou A, Zoras S, Iordanidis A (2021c) Fuel quality index and fuel quality label: two versatile tools for the objective evaluation of biomass/wastes with application in sustainable energy practices. Environ Technol Innov 23:101739. https://doi.org/10.1016/j.eti.2021.101739

Vasileiadou A, Papadopoulou L, Zoras S, Iordanidis A (2022) Development of a total ash quality index and an ash quality label: comparative analysis of slagging/fouling potential of solid biofuels. Environ Sci Pollut Res 29:42647–42663. https://doi.org/10.1007/s11356-021-18225-4

World Bank (2018) What a waste 2.0: a global snapshot of solid waste management to 2050, 2020. World Bank. https://doi.org/10.1596/978-1-4648-1329-0

Zhu J-J, Park D, Chang DT, Cheng C, Anderson PR, Fan H-J (2021) Unsupervised aided investigation on the associations between municipal solid waste characteristics and socio-economic conditions. Environ Res 194:110633. https://doi.org/10.1016/j.envres.2020.110633